

T.R.
GEBZE TECHNICAL UNIVERSITY
GRADUATE SCHOOL OF NATURAL AND APPLIED SCIENCES

**INCREASING THE CORROSION RESISTANCE OF
GALVANIZED LOW CARBON STEELS WITH GRAPHENE
REINFORCED POLYMER COATINGS**

SAMET BERK AKTÜRK
**A THESIS SUBMITTED FOR THE DEGREE OF
MASTER OF SCIENCE**
DEPARTMENT OF MECHANICAL ENGINEERING

GEBZE
2021

T.R.
GEBZE TECHNICAL UNIVERSITY
GRADUATE SCHOOL OF NATURAL AND APPLIED SCIENCES

**INCREASING THE CORROSION
RESISTANCE OF GALVANIZED LOW
CARBON STEELS WITH GRAPHENE
REINFORCED POLYMER COATINGS**

SAMET BERK AKTÜRK
**A THESIS SUBMITTED FOR THE DEGREE OF
MASTER OF SCIENCE**
DEPARTMENT OF MECHANICAL ENGINEERING

THESIS SUPERVISOR
ASSOC.PROF.DR. AHMET SİNAN ÖKTEM

GEBZE
2021

T.C.
GEBZE TEKNİK ÜNİVERSİTESİ
FEN BİLİMLERİ ENSTİTÜSÜ

GALVANİZLİ DÜŞÜK KARBONLU
ÇELİKLERİN GRAFEN TAKVİYELİ
POLİMER KAPLAMALAR İLE KOROZYON
DİRENCİNİN ARTTIRILMASI

SAMET BERK AKTÜRK
YÜKSEK LİSANS TEZİ
MAKİNE MÜHENDİSLİĞİ ANABİLİM DALI

DANIŞMANI
DOÇ. DR. AHMET SİNAN ÖKTEM

GEBZE

2021

GEBZE TEKNİK ÜNİVERSİTESİ	YÜKSEK LİSANS JÜRİ ONAY FORMU
----------------------------------	--------------------------------------

GTÜ Fen Bilimleri Enstitüsü Yönetim Kurulu'nun 01/07/2021 tarih ve 2021/30 sayılı kararıyla oluşturulan jüri tarafından 13/07/2021 tarihinde tez savunma sınavı yapılan Samet Berk AKTÜRK'ün tez çalışması Makine Mühendisliği Anabilim Dalında YÜKSEK LİSANS tezi olarak kabul edilmiştir.

JÜRİ

ÜYE

(TEZ DANIŞMANI) : DOÇ. DR. AHMET SİNAN ÖKTEM

ÜYE

: DR. ÖĞRETİM ÜYESİ RECEP ÖNLER

ÜYE

: PROF. DR. AYŞE BEDELOĞLU

ONAY

Gebze Teknik Üniversitesi Fen Bilimleri Enstitüsü Yönetim Kurulu'nun

...../...../..... tarih ve/..... sayılı kararı.

İMZA/MÜHÜR

SUMMARY

Due to their superior chemical and mechanical properties, graphene and graphene oxide have recently emerged as filler materials in various coating systems to improve corrosion resistance and mechanical durability. These unique characteristics make them favorable for the formation of a passive layer to protect metals from oxidation and corrosion. In this study, a multilayer protective coating is obtained on a low carbon steel substrate, and the corrosion resistance of this coating is investigated via potentiodynamic polarization. To obtain the multilayer coating system, the samples are first galvanized and then passivized. With the optimized new coating method, thin layers of two different primers are applied to the passivation layer, followed by a polyamide 12 (PA12) topcoat layer with a controllable thickness. The effects of reduced graphene oxide filler on primers are experimentally investigated with 0.5 %wt. filler rate. Cross-sections of coated specimens are examined via SEM and EDS. Experimental corrosion rates for coated specimens are examined in an aqueous 3.5% NaCl solution by the Tafel method. It is shown that the corrosion rates are reduced to one in 10 with the 0.5 % wt. addition of reduced graphene oxide as a filler material in primer layers in the multilayer coating system. These results show that graphene reinforced polymer composite coatings can be an alternative protection method against corrosion for many engineering applications.

Key Words: Reduced Graphene Oxide, Thin Film Coating, Corrosion, Composite Coating.

ÖZET

Üstün kimyasal ve mekanik özellikleri nedeniyle, grafen ve grafen oksit, çeşitli kaplama sistemlerinde korozyon direncini ve mekanik dayanıklılığı arttırmak için yakın zamanda dolgu malzemeleri olarak ortaya çıkmaktadır. Bu eşsiz özellikler, metalleri oksidasyon ve korozyondan korumak için pasif bir tabaka oluşturarak onları uygun hale getirir. Bu çalışmada, düşük karbonlu çelik bir alt tabaka üzerinde çok katmanlı bir koruyucu kaplama elde edilmiş ve bu kaplamanın korozyon direnci potansiyodinamik polarizasyon ile araştırılmıştır. Çok katmanlı kaplama sistemini elde etmek için, numuneler önce galvanizlenmiş daha sonra pasifleştirilmiştir. Optimize edilmiş yeni kaplama yöntemiyle, pasivasyon katmanına iki farklı astardan oluşan ince katmanlar ve ardından kontrol edilebilir bir kalınlığa sahip poliamid 12 (PA12) son kat katmanı uygulanır. İndirgenmiş grafen oksit dolgu maddesinin primerler üzerindeki etkileri, ağırlıkça %0,5 dolgu oranı ile deneysel olarak araştırılmıştır. Kaplanmış örneklerin kesitleri, SEM ve EDS ile incelenmiştir. Kaplanmış örnekler için deneysel korozyon oranları, Tafel yöntemi ile sulu %3,5 NaCl çözeltisi içinde incelenmiştir. Çok katmanlı kaplama sistemindeki tabakaların astar kaplamalarına dolgu maddesi olarak ağırlıkça %0,5 indirgenmiş grafen oksit ilavesi ile bile korozyon oranlarının 10'da bire düştüğü gösterilmiştir. Bu sonuçlar grafen takviyeli polimer kompozit kaplamaların birçok mühendislik uygulaması için korozyona karşı alternatif bir koruma yöntemi olabileceğini göstermektedir.

Anahtar Kelimeler: İndirgenmiş Grafen Oksit, İnce film kaplama, Korozyon, Kompozit kaplama

ACKNOWLEDGEMENTS

I would like to express my deep and sincere gratitude to my supervisor, Assoc. Prof. Ahmet Sinan ÖKTEM, who not only shared his profound scientific knowledge with me but also taught me great lessons of life. His support, suggestions, and encouragement gave me the drive and will to complete this work.

I am also indebted to Asst. Prof. Recep Önler, who also guided me during my research with his much valuable advice. I acknowledge his contribution by generously devoting time and proving insightful comments to my studies during my master's degree.

I would also like to gratefully thank Assoc. Prof. Mustafa Fazıl Serincan, Prof. Ümit Demir and Ogun Bora Saban for the assistance of corrosion tests, and to Ahmet Nazım and Adem Şen for the analysis of SEM and TEM. Additionally, thanks to Mr. Erdal Topaç with Hazerfen Kimya Malzeme ve Enerji Teknolojileri Sanayi Ticaret A.Ş. for valuable suggestions help in all stages of this research.

This work was performed with support from Bant Boru Company. I would like to acknowledge all the parties who made this project possible.

Last but not least, I owe my deepest gratitude to my mother, my father, and also my brothers Furkan, Batuhan for their unconditional love. I am deeply thankful to my sister Nihal for her endless support.

TABLE of CONTENTS

	<u>Page</u>
SUMMARY	v
ÖZET	vi
ACKNOWLEDGEMENTS	vii
TABLE of CONTENTS	viii
LIST of ABBREVIATIONS and ACRONYMS	ix
LIST of FIGURES	xi
LIST of TABLES	xiii
1. INTRODUCTION	1
1.1. Corrosion	1
1.2. Protective Coatings	4
1.3. Graphene	5
1.4. Literature Review	6
1.5 Objective and Content of Thesis	8
2. METHODOLOGY	10
2.1. Sample Preparation	11
2.2. Chemical Conversion and Primer Coatings	13
2.3. Polyamide Powder Preparation	21
2.4. Polyamide 12 Coating	24
3. MICROSTRUCTURE ANALYSIS	27
4. CORROSION TEST	29
5. RESULTS AND DISCUSSIONS	31
6. CONCLUSIONS AND FUTURE WORKS	40
7. PUBLICATIONS FROM THESIS	41
REFERENCES	42
BIOGRAPHY	48

LIST of ABBREVIATIONS and ACRONYMS

<u>Abbreviations</u>	<u>Explanations</u>
<u>and Acronyms</u>	
GDP	: Gross Domestic Product
U.S.	: United States
CVD	: Chemical Vapor Deposition
Cu	: Copper
Ni	: Nickel
mm	: Millimeter
nm	: Nanometer
μm	: Micrometer
Cr	: Chromium
SiO ₂	: Silicon Dioxide
NiTi	: Nitinol
H ₂ O ₂	: Hydrogen Peroxide
HNO ₃	: Nitric acid
°C	: Celsius
rpm	: Revolutions Per Minute
min	: Minute
PA12	: Polyamide 12
G	: Gram
ml	: Milliliter
hrs	: Hours
L	: Liter
wt	: Weight
SEM	: Scanning Electron Microscope
EDS	: Energy Dispersive Spectroscopy
FTIR	: Fourier-Transform Infrared Spectroscopy
Ag	: Silver
AgCl	: Silver Chloride
NaCl	: Sodium Chloride

cm ²	:	Square Centimeter
MV	:	Millivolt
GO	:	Graphene Oxide
E _{corr}	:	Corrosion Potential
I _{corr}	:	Corrosion Current Density
RGO	:	Reduced Graphene Oxide
TPa	:	Tera Pascal

LIST of FIGURES

<u>Figure No:</u>	<u>Page</u>
1.1: Rust, the most familiar example of corrosion.	1
1.2: The result of corrosion of metallic iron.	2
1.3: Crystallographic structure of graphene	6
1.4: PA12 coated pipes.	9
2.1: Layers of coating.	10
2.2: Flow chart for coating processes.	11
2.3: Galvanized low carbon steel.	12
2.4: Granodine coated galvanized low carbon steel.	14
2.5: The primer-coated samples obtained with 75% primer in the mixture and 2 repetitions.	16
2.6: Flow chart for chemical conversion and primer coating processes.	16
2.7: a) The sample is attached to the overhead stirrer. b) The sample is rotated at 100 rpm.	17
2.8: a) The sample is removed from granodine. b) The sample is rotated at 1000 rpm.	18
2.9: The drying process in the oven.	19
2.10: The sample coating with a primer.	19
2.11: Primer and chemical conversion coated low carbon steel.	20
2.12: a) PA12 is melted in formic acid. b) The melted PA12 is poured into a container.	21
2.13: a) Dried PA12. b) Grounded PA12.	22
2.14: a) Separating ethanol from the mixture. b) PA12/Water dispersion is prepared.	23
2.15: a) The dispersion is poured into recess. b) The dispersion is spread.	24
2.16: The excess dispersion is discarded	25
2.17: The sample is dried in the oven.	25
2.18: a) Single-layer PA12 coating. b) Double-layer of PA12 coating	26
3.1: Coating layers.	27

3.2:	Mounted specimens in bakelite resin.	28
4.1	Corrosion test setup	29
4.2	Corrosion process showing anodic and cathodic components of total current.	30
5.1	Chemical composition with SEM-EDS.	31
5.2:	SEM results of primer-coated samples.	32
5.3	Coating failures.	33
5.4	Coating failures.	33
5.5	SEM results of 4 different sample sections.	34
5.6	SEM results of 4 different sample sections with different dispersion ratios.	35
5.7	FT-IR patterns of melted PA12	36
5.8	FT-IR patterns of dissolved PA12 in formic acid.	36
5.9	FT-IR patterns of washed PA12 in ethanol.	37
5.10	FT-IR patterns of RGO-PA12 composite.	37
5.11	Tafel polarization curves.	38

LIST of TABLES

<u>Table No:</u>	<u>Page</u>
2.1: Variant parameters for the developed coating technique.	15
5.1: Corrosion test results.	39

1. INTRODUCTION

1.1. Corrosion

Corrosion is a natural degrading process that leads to material losses due to chemical interactions with its environment [1]. These electrochemical reactions can be defined as charge-transfer processes that occur between the metallic surface and an aqueous solution. The anodic reaction in which electrons are released and the cathodic reaction, which is the opposite of anodic reaction, occur at equivalent rates and simultaneously [2].



Figure 1.1: Rust, the most familiar example of corrosion [7].

In many domestic systems and industrial processes, corrosion can cause problems such as premature failures, and degradation [3]. Depending on its mechanism and surface, corrosion can occur in different forms, and its predictability and controllability may differ. Uniform corrosion, pitting, crevice corrosion, galvanic corrosion, erosion, intergranular, and stress corrosion cracking are some of the main forms of corrosion attack [4]. For example, stress corrosion cracking occurs in the

presence of tensile stress and a corrosive medium, and fine cracks progress through the surface [4]. On the other hand, the relative motion between a corrosive liquid and a metal surface can cause erosion-corrosion in a short time. Crevice corrosion is a form of localized corrosion within crevices on metal surfaces. The rust shown in figure 1.1 is an example of uniform corrosion and causes the greatest metal weight loss. The surface of the iron acts as the anodic site and oxidizes while oxygen is reduced to water at the cathodic site. The following chemical equation represents its reactions:

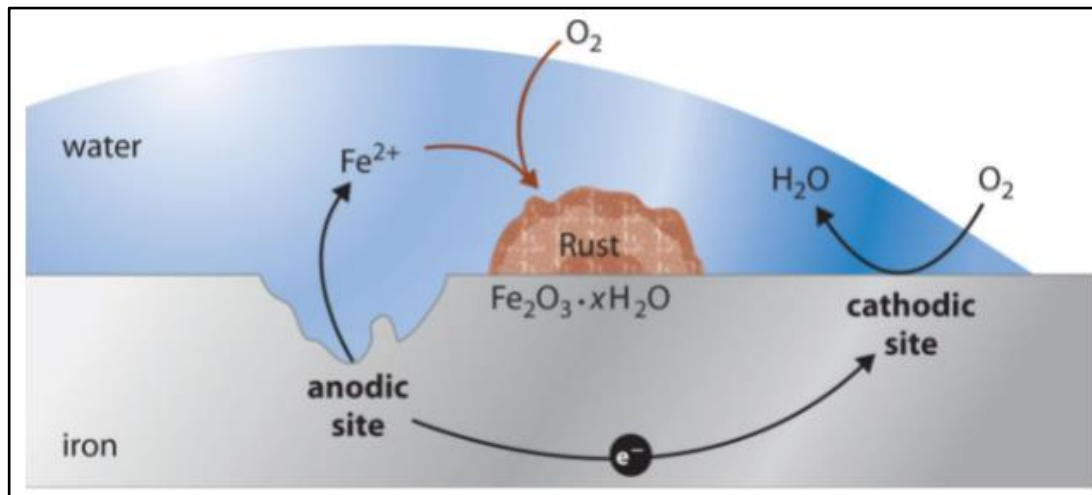
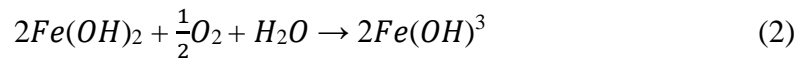
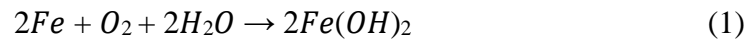


Figure 1.2: The result of corrosion of metallic iron [5].

It may appear safe to say that most people are familiar with corrosion and its types, but the social and economic effect of corrosion still takes a crucial role than expected. At least the economic effect of this material degrading process is expensive enough to be a significant motivation for most of the current corrosion research, which has the potential to contribute to other fields of science and engineering [6].

According to a recent study, the total annual estimated global cost of corrosion to be \$276 billion in the United States (U.S.), which accounts for 3.1% of the gross domestic product (GDP) [8]. When compared to Turkey's GDP of \$934,2 billion in

the same year, a total loss of corrosion can be estimated \$28,9 billion for Turkey. Even if the sectors for the source of the corrosion may not be the same in the US and Turkey, the total annual corrosion loss of about \$30 billion poses a major problem [9]. On the other hand, it is expected that saving some of the cost of corrosion can be realized by using available corrosion control practices. The researchers' study estimated that 25 to 30% of this total annual corrosion cost in the U.S. may be avoided if currently available corrosion technology is effectively employed [8]. This shows that the prevention of the corrosion loss of about \$10 billion annually may be possible in Turkey.

Despite corrosion control practices that have improved over the past several decades, corrosion is a natural process that cannot be completely prevented, it can only be minimized. Researchers have been trying to minimize these material losses, as well as the concomitant economic losses, that are derived from automobiles, drinking water systems, home appliances, pipelines, bridges, and public buildings, etc. to prevent this dangerous and expensive damage of the corrosion. There are different leading methods to prevent corrosion. Case hardening, diffusion treatment, conversion coating, cathodic and anodic protection are some of them. For example, with hot-dip galvanizing, which is one corrosion protection method, metal parts are coated with a well-adhered zinc-steel alloy to prevent corrosion. On the other hand, diffusion treatment is a good example of corrosion protection methods. The surface layers are enriched by diffusing atoms of a different material at high temperatures and improve the surface characteristics such as corrosion resistance. More and better ways are needed to control and retard corrosion and improve optimal practices. Therefore, one of the most economical and effective procedures used to overcome this issue is to cover the surfaces with coatings [10]. It is expected that by developing protective coatings with the least changes in the physical properties of the surface, the above losses can be abated [3]. It was also predicted that \$121 billion, which is 1.38% of the U.S. GDP, was spent on the total direct cost of corrosion control services in the U.S., and 88.3% of this cost was related to organic coatings [8]. These results prove the importance of corrosion control methods to reduce the costs of maintenance and increase the expected life of a structure. Among other existing methods, corrosion protective coatings are gaining popularity as they are cheap and effective [11].

1.2. Protective Coatings

Surface coatings have been used for both decorative and protective purposes since ancient times and they can be classified as organic, inorganic, and metallic coatings in themselves [12]. Coatings designed for corrosion protection must be able to provide an effective physical barrier, which impedes access of aggressive species to the metallic interface [13]. In addition, the coatings must possess intrinsic durability, good adhesion to the substrate, sufficient flexibility, and toughness to withstand impacts and cracking while maintaining their appearance when subjected to stress, swell, mechanical abuse, or weathering [14]. According to the conditions of use, these types of coatings can be exposed to different corrosion risks, and they can also be used as a single layer or in a multi-layer coating system. Specific applications may require other coating properties as well. For example, galvanizing is one of the most widely used sacrificial methods for metallic coating [64]. This method which is comprised of applying metallic zinc to carbon steel for corrosion can provide cathodic protection. On the other hand, conversion coatings, one of the examples of inorganic coatings, offer enhanced surface hardness and protect the surface from further corrosion with the help of produced an adherent corrosion product. However, on a weight basis, organic coatings protect more metal than any other corrosion protection method [15]. According to the U.S. Department of Commerce, in 1997, \$16.56 billion of organic coating material was sold in the U.S. and with approximately one-third of the total sales for the main purpose of corrosion protection [8]. For this purpose, protective coatings have become most widely used to protect a surface from an aggressive environment [16]. Instead of using a single type of layer coating, multifunctional systems that combine more than one type of coating are preferred for these corrosion control purposes. Thus, multilayer coatings combine the best properties of single layers. Therefore, these coatings can also provide other requirements such as durability, chemical inertness, resistance to thermal fluctuation.

Nanocomposites, hydrophobic coatings, and organic-inorganic hybrid coatings have already emerged in extending the life of various materials in corrosive environments [17]. In the future, the demand for composite coating materials with high corrosion resistance may increase, depending on environmental factors and performance, as well as techniques derived from improved experimental studies. Materials are incorporated into the polymer composites as a filler to enhance corrosion performance and obviate the lack of polymer coatings [18-19-20]. Especially, for the last years, instead of expensive or ineffective coating materials, new innovative materials have been tested, and graphene has been one of the most favored of these materials [21-12-23]. Besides, composite coatings, involving graphene derivatives, have been used and tested in many recent studies and seem to be one of the indispensable materials for protective coatings [24-25-26].

1.3. Graphene

Graphene is one atomic thickness of graphite and it is the first known two-dimensional form of sp² bonded carbon atoms [27-28]. Its crystallographic structure is shown in Figure 1.3. Since its discovery, the research wave on graphene is getting higher and higher due to outstanding mechanical, chemical, thermal properties, and functionalized capabilities [29-30]. Graphene has also unique qualities such as exceptional thermal conductivity (5000 Wm⁻¹K⁻¹), high electron mobility (250,000 cm²/Vs) at room temperature, and superior mechanical properties with Young's modulus of 1 TPa [31-32-33-34]. These unique characteristics make graphene one of the most favorable materials in both scientific and industrial fields such as automotive, aerospace, and marine.

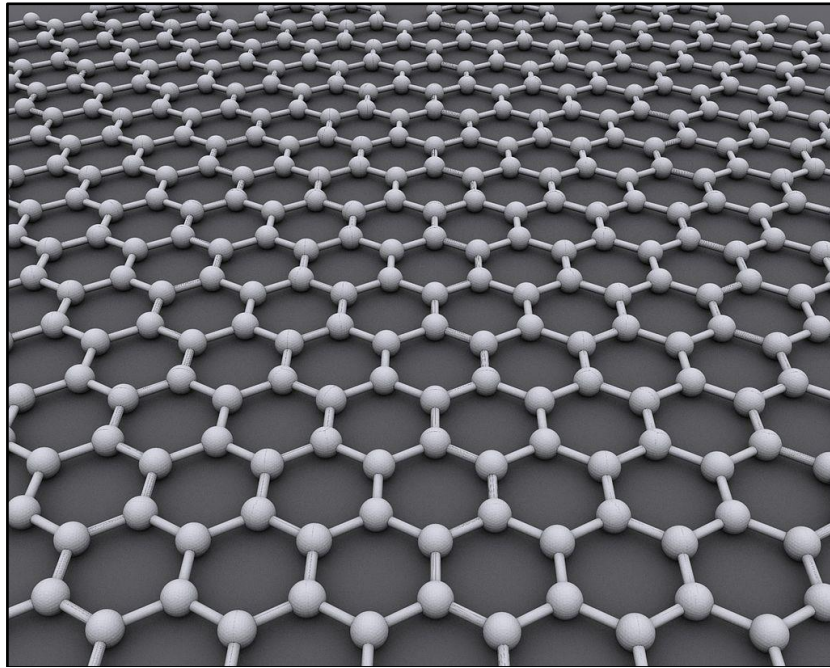


Figure 1.3: Crystallographic structure of graphene [27].

Recently, there are many studies on applications in various fields such as sensors, photodetectors, solar cells, polymer composites, energy storage devices [35-36-37]. Especially, polymer nanocomposites with graphene derivatives have a remarkable effect on high-performance protective coatings [38-39-40]. Anti-corrosive coatings with the usage of graphene-based composites are an emerging trend [11]. Graphene-reinforced polymer nanocomposite system gives enhanced anti-corrosion ability to coatings primarily because of the following protection mechanisms: (i) homogeneous distribution of polymer phase on the substrate's surface resulting in the formation of smooth and uniform passive layer, (ii) limiting the penetration and providing tortuous diffusion path to the corrosive agents along with the coating thickness and (iii) reformed mechanical strength to resist cracks and improved adhesion ability to the metal surface [41]. The main driving force behind this trend is the need for more effective anti-corrosive coating methods to extend the life of the surface coatings and reduces the cost [42-43].

1.4. Literature Review

Recently, several studies on corrosion-resistance coatings with graphene and graphene derivatives have been applied on different substrates. [44-45] The

substrates such as alloys, carbon steel, copper, nickel, and stainless steel can be used for these studies. Prasai et al. studied that anti-corrosive coatings with pure graphene layers obtained by chemical vapor deposition (CVD) method on copper and nickel, they have 7 times better corrosion performance than bare copper and 20 times better than bare nickel [46]. As well as substrates, the coating technique is also an important parameter for corrosion resistance. Prasai also compared the corrosion resistance of multilayer graphene coatings which are obtained by the CVD method and the mechanical transfer method. It was found that the multilayer graphene coating directly obtained by CVD has 20 times higher corrosion resistance than bare nickel, while the multilayer coating obtained by the mechanical transfer method has 4 times greater corrosion resistance than bare nickel because of the corrosion transport path left during the transformation [44-47]. The number of layers can also have a positive effect on corrosion resistance in some specific cases. Olia et al obtained coatings containing different numbers of layers and the same total thickness on steel, the results prove that multilayered coatings with more different layers provide more resistance against corrosion compared to others [48]. At the same time, the preparation of multilayer graphene coatings can be a simple and effective method to solve the corrosion problem, because the mutually matching defects overlap with each other and a spatial steric hindrance is formed [49]. This provides us long-term corrosion protection which is quite important for most polymer nanocomposite coatings. On the other hand, the corrosion performance of the zinc-rich coating can be increased by the barrier behavior of graphene nanosheets [50-54-52]. Zhou et al. report that epoxy zinc-rich coating with graphene oxide coating exhibited better corrosion performance than a pure zinc-rich coating due to the positive impermeability [53]. The coating method is also important to create a uniform, robust oxidation, and crack-free coating. Sing developed a coating with excellent microstructure and controlled thickness (40nm) on the copper. With this study, the reduction in the corrosion rate of the copper is observed 10 times better and it has excellent adherence to the metal surface [54]. Sun and coworkers reveal that graphene-SiO₂ composites enhance corrosion resistance when embedded into an anti-corrosive coating [55]. Impermeability is also an important feature that affects the corrosion resistance of materials. In this respect, Bunch et al. showed that graphene film may prevent the gas molecules from transferring by van der Waals force between graphene and SiO₂ [56]. Another experimental study reports that cold-rolled

steel, used for industrial setup, is developed with a reduced graphene oxide coating and better anti-corrosive performance is observed. This report shows that some applications of reduced graphene oxide coatings on cold-rolled steel sheets can be possible in an industrial setup [57]. Chang et al. improve anti-corrosive coating with polyaniline/graphene composite and, Yu and coworkers investigated graphene oxide derivatives incorporated in epoxy coatings [58-59]. Chen et al. and Cho et al. used graphene in the CVD system and proved that it can provide corrosion resistance for Cu and Cu/Ni alloys [59-60]. Podila et al. reported that the graphene-coated part of a Cu coin exposed to H₂O₂ remained protected from oxidation while the uncovered region is discolored [61]. They also immersed graphene-coated NiTi in 70% HNO₃ to confirm the durability of graphene coatings. According to Raman spectroscopy, there was no change in the G- band frequency referring that the graphene coating was extremely durable. Zhang et al. suggest that graphene coating can also be used for some biomedical applications such as metal implants. They demonstrated that graphene can effectively prevent the toxicity of copper by inhibiting corrosion [62].

The coating materials, substrates, coating techniques, number of coating layers, and thicknesses are significant parameters that can affect the rate of corrosion, and some research on these topics are given above. Above mentioned studies show that with the usage of sufficient graphene and derivatives in especially polymer coatings, anti-corrosive performance, and barrier properties can be remarkably improved which leads to cost-effective and long-term corrosion protection.

1.5. Objective and Content of Thesis

Recently, several studies have focused on examining the effect of graphene in polymer coatings and its contribution to surface barrier properties. Some of them have already been mentioned in the literature review. However, there is a scarcity of research that investigates the role of graphene and its derivatives with reinforced polymer coatings on corrosion resistance. Despite some challenges, it is an ongoing effort to apply graphene polymer composites in the industry. And there are still many limitations in industrial applications for graphene coatings even those that have good mechanical properties.

In this thesis, we aimed to develop, the anti-corrosive graphene-based multilayer polymer coating on the steel substrate. For this purpose, a multilayer coating system containing galvanization layer, conversion coating layer, primer, and topcoat are applied on a steel substrate with a controlled thickness of individual layers with and without reduced graphene oxide in the primer layer. The microstructure of each coating is analyzed. The corrosion performance of the prepared samples is investigated by the electrochemical test method. The experimental coating procedure that allows obtaining desired thicknesses throughout the target surface is studied. It is shown that the addition of sufficient RGO can increase corrosion resistance.



Figure 1.4: PA12 coated pipes [63].

2. METHODOLOGY

The first aim of this thesis is to develop a protective and durable polymer composite coating with a controllable thickness on top of a low carbon steel plate. The second aim is to increase the corrosion resistance of this polymer coating by adding graphene derivatives. For these purposes, a coating consisting of many layers is obtained on galvanized low carbon steel as shown in Figure 2.1. This coating consists of layers which are galvanizing, passivation, conversion coating, primer coating, and topcoat PA12. The corrosion resistance of this low carbon steel is increased with graphene reinforced primer coating.

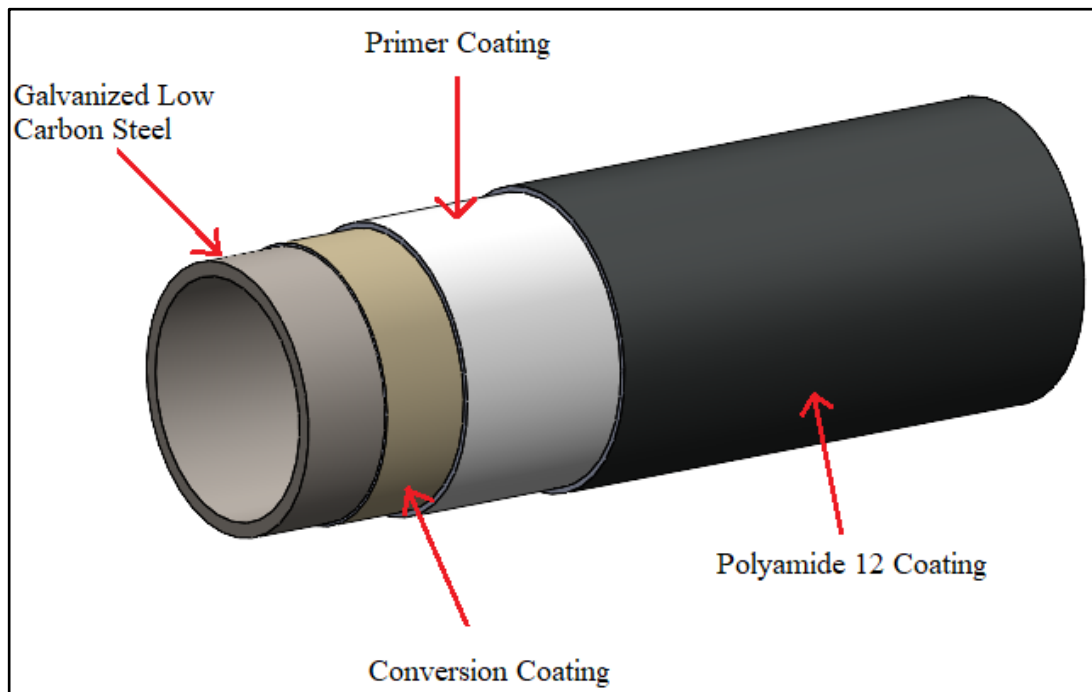


Figure 2.1: Layers of coating.

The coating materials, substrates, pre-cleaning, and coating processes are preferred according to the facilities in the laboratory. In this regard, a plate substrate is used, and a new coating technique is developed.

2.1. Sample Preparation

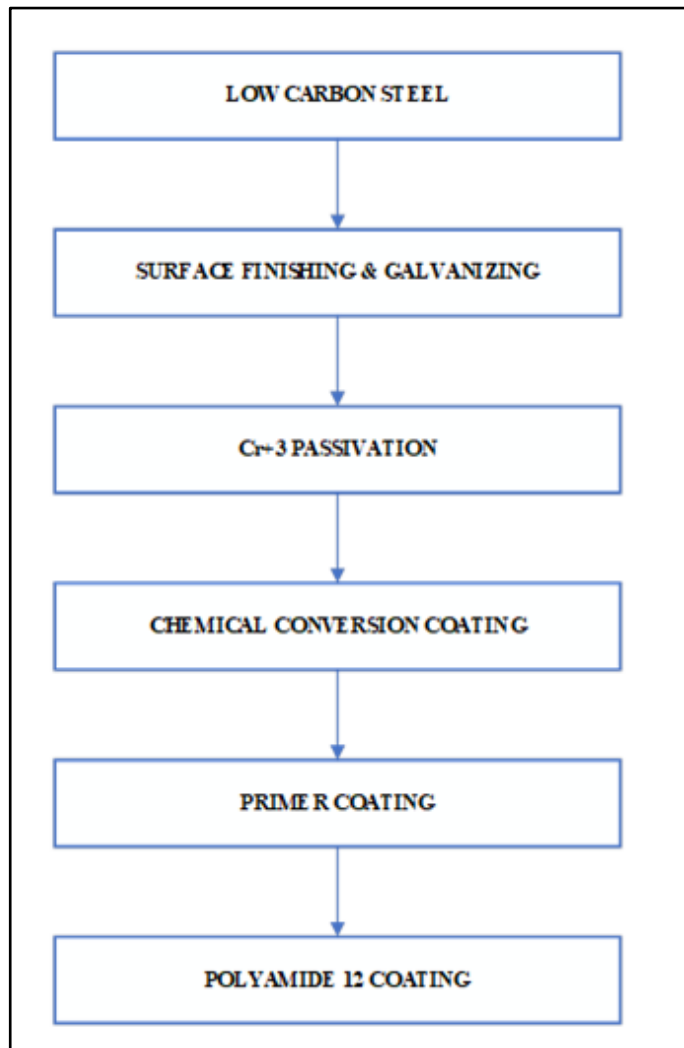


Figure 2.2: Flow chart for coating processes.

Figure 2.2 shows the coating processes used in this work. It includes the sample preparation steps and shows all single layers in the coatings. Low carbon steel that is cut in a square (70x70 mm) with 3 mm thickness is used as a substrate which is designed according to the coating methods. The size of the samples to be coated is also chosen following our corrosion measurement method. Two holes are drilled from the opposite diagonal of the square sheets. Then, plates are engraved to create a 200 μm deep recess with precision machining. The holes help to attach the overhead stirrers which will be used to coat primers and the recess helps to topcoat

the sample with PA12. These sample preparations are revised to adapt to the coating methods used.

The samples are prepared with the traditional polymer coatings approach as surface finishing and cleaning. Before galvanizing, some pretreatment processes are applied such as electrolytic cleaning steps. Following cleaning operations of the sample, they are galvanized with electroplating. Electro galvanization is one of the most popular anode coatings which provides easy fabrication with low cost and it is used for preventing corrosion for steel. [64]. Especially if chromate 3 is applied over the galvanizing to promote paint adhesion, an overlying paint coating may have a longer life with this Zn coating [64]. It can be used in multifunctional coating systems which are preferred by many industries such as automobile and defense. Thus, this chromium conversion coating called passivation is also preferred to apply to our galvanized samples. Trivalent chromium-based coatings started to be frequently used in surface finishing industries after hexavalent chromium was prohibited [65]. In addition, in this thesis, Cr+3 passivation is preferred which also provides good corrosion resistance and increases surface hardness. The galvanized low-carbon steel is shown in Figure 2.3.



Figure 2.3: Galvanized low carbon steel.

2.2. Chemical Conversion and Primer Coatings

The chemical conversion coating which is a part of an overall coating process is applied to galvanized low carbon steel to improve the transition between the substrate and primer. They have been preferred for providing adhesion and corrosion protection of the coating systems in industrial applications for years [64]. Thus, it is an important step itself in the anti-corrosive performance of the multilayer coating system. It is kind of a dry-in-place chromium-free treatment for aluminum, zinc, zinc alloy, and cold-rolled steel surfaces and it produces a uniform coating that inhibits corrosion and increases the durability of paint finishes [67]. The chemical conversion layer is placed between the galvanized low carbon steel and the primer layer in our multilayer coating system.

In this thesis, recommended pre-cleaning processes for Granodine by Henkel used as chemical conversion coating material are applied [66]. As usual, all samples must be free of grease, oil, rust, scale, and other matter before applying the chemical conversion coating layer. Even if samples are carefully cleaned with ethanol, these matters should be taken into consideration when selecting galvanized samples. Because there may already be samples that have problems on the coating surface from the previous coating steps (galvanization and passivation), and that may adversely affect the next coating steps. It is more reliable to obtain a multi-layer coating system by selecting the samples that do not contain exceptional surface coating problems after each single layer coating step. After cleaning with ethanol, the samples are rinsed thoroughly with distilled water. Then, the coating surface is cleaned by spraying the air with the help of a compressor to keep the surface free from contamination. For the last step of the pre-cleaning process, samples are left to dry in the oven to get ready for the chemical conversion coating step [66]. The granodine coated galvanized low carbon steel is also shown in Figure 2.4.

In the multi-layer coating system that is desired to be obtained, the next step after Granodin coating is the primer coating. The primers are generally used to make the surface suitable for the topcoats and facilitate the adhesion over a variety of surfaces no matter what is used for the substrate [68].

In this study, a polyamide-based primer by AkzoNobel is preferred as a primer coating material. To obtain a better coating performance with the novel coating method developed, this primer material is diluted in certain proportions with thinner before it is used for coating. During the whole process, alcohol or derivatives are not used for pre-cleaning or post-processes of the primer coating. Because it is observed that chemical conversion and primer coating materials are dissolved in these kinds of solvents and therefore the coatings are damaged. So, only distilled water is used as a pre-cleaning process after granodine coating. Then, the coating surface is cleaned again by spraying the air before primer coating. The primer layer is the last coating material of the system before the topcoat.

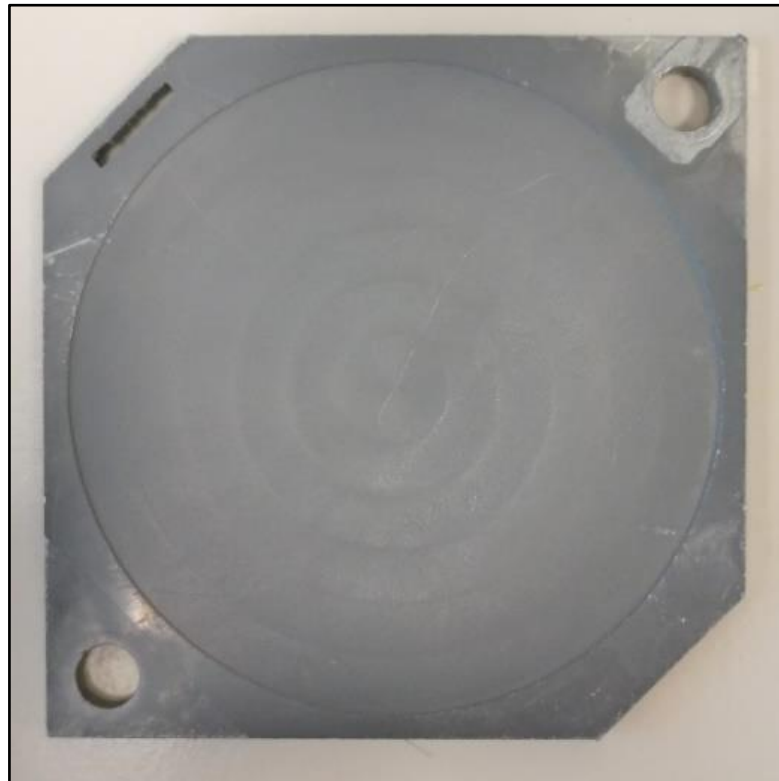


Figure 2.4: Granodine coated galvanized low carbon steel.

Generally, some traditional coating techniques such as spin and dip coating methods are preferred for chemical conversion and primer coating materials on metal surfaces. Preferred coating techniques may differ for different applications depending on their requirements, advantages, and disadvantages. In this study, similar coating techniques were tried, but the desired coatings with a uniform and controllable thickness may not be obtained due to some limitations of the laboratory

facilities and coating materials. So, within the bounds of possibilities, a new coating method has been developed that gives acceptable results. While developing this coating technique, its suitability to laboratory conditions, controllability of coating thickness, adaptability to the relevant coating materials and substrates were taken into consideration. As the coating processes progress, this technique has also been optimized and improved according to the results obtained. Therefore, while the rotation speed and duration of the samples are considered invariant parameters, the number of process repetitions and dilution rate of primer material are considered as variant parameters for the developed coating technique shown below. In this respect, the number of process repetitions of 1, 2, 3, and the dilution ratios of primer material of 25%, 50%, 75% are examined.

Table 2.1: Variant parameters for the developed coating technique.

Number of process repetitions	Dilution ratios of primer material
1	25%
2	50%
3	75%

When the number of process repetitions was 1, it was observed that the primer material did not penetrate the substrate well and there were some uncoated areas on the surface observed. Besides, it was determined that sufficient coating thickness was obtained according to scanning electron microscopy results, and these uncoated areas disappear while the number of repetitions of the process was 2. It was decided that 3 repetitions were unnecessary. On the other hand, when 75% primer was preferred in the mixture of thinner primer, it was spread evenly over the coating surface and a more stable coating appearance than 25% and 50% were obtained in repeated coatings.

According to SEM results, it was decided to prefer 75% wt of primer in the mixture, and a 2-repetition process was used. Some coating studies with these determined parameters are shown in Figure 2.5.



Figure 2.5: The primer-coated samples obtained with 75% primer in the mixture with 2 repetitions.

The chemical conversion and primer coating methods used in the thesis were developed indirectly based on the principles of spin and dip coating techniques. It is kind of a combination of these two techniques. The flow chart for chemical conversion and primer coating is shown in Figure 2.6.

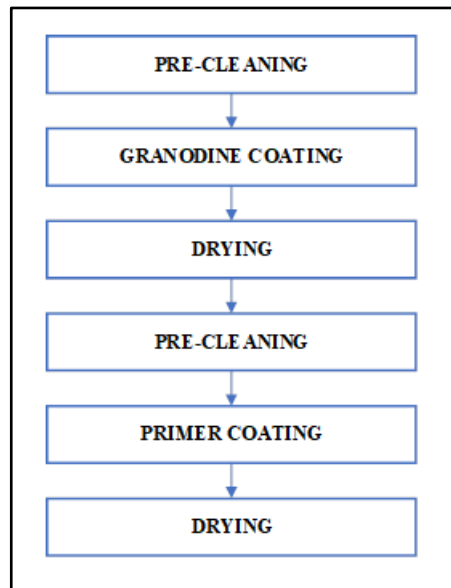


Figure 2.6: Flow chart for chemical conversion and primer coating processes.

The steps of this modified and optimized new coating process are shown below. An overhead stirrer is used to provide spin and dip movements to the sample in the coating. The sample is attached to the overhead stirrer through the pre-drilled hole in the coating. The sample is attached to the overhead stirrer through the pre-drilled hole with the help of screws and a designed rod after the pre-cleaning processes described above.

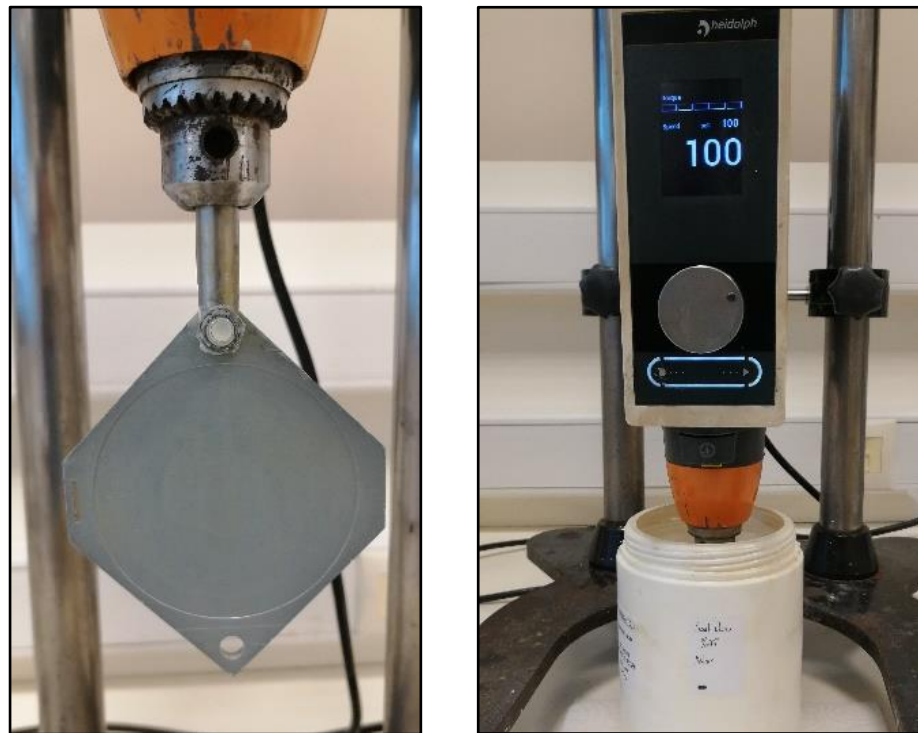


Figure 2.7: a) The sample is attached to the overhead stirrer b) The sample is rotated at 100 rpm.

At this stage, one of the diagonals of the sample is aligned perpendicular to the ground as shown in Figure 2.7 (a). Another important point to note is that the sample is fixed securely to the rod so that it does not move out of place during the rotations. Otherwise, in addition to the risk of accident, a smooth and well-spread coating may not be obtained if a stable movement is not achieved. A container filled with granodine to immerse the sample is placed under the stirrer. Then, the sample is carefully immersed in that container, especially, the recess on the surface should be completely submerged into the granodine. After immersion is completed, the overhead stirrer is set to 100 rpm and operated while the sample is still in the container as shown in Figure 2.7 (b).



Figure 2.8: a) The sample is removed from granodine b) The sample is rotated at 1000 rpm.

The submerged sample is gently removed from the granodine after 1 minute of rotating at 100 rpm. The aim here is to remain the substrate in the solution for a while and the granodine deposits well itself on the recess during rotation. Next, an empty container is replaced under the stirrer and the sample is rotated for 1 more minute inside of that when the stirrer is set to 1000 rpm this time. The aim of this is to drain the excess chemical conversion coating material from the sample and ensure that coating is spread evenly on the surface with the help of this high rpm value. This whole process is repeated one more time from beginning to end to get rid of defects and make sure the solution penetrates the surface thoroughly. This step is also shown in Figure 2.8.



Figure 2.9: The drying process in the oven.

After these repetitive processes are finished, the coated sample is carefully removed from the overhead stirrer and left to dry in the oven at 60 °C for 15 min as recommended [66]. It is paid attention that the coated parts of the samples do not encounter any place during the whole process.



Figure 2.10: The sample coating with a primer.

After granodine coatings are completed by the drying process, the samples are prepared for primer coating as described above. Then, the same coating processes are applied to the samples with the primer coating material which is diluted with thinner. The rotation speeds, durations, repetitions, and drying processes of the samples are completely the same as the granodine coating. By this optimized novel coating method, two different coatings both granodine and primer are obtained with their desired coating properties. One of the coated samples is shown in Figure 2.11. Lastly, reduced graphene oxide reinforced primer coating with 0.5% wt filler rate is prepared with the same method to investigate the effect of graphene on corrosion resistance. In this regard, rGO reinforced primer material is prepared. Firstly, the thinner and rGO are treated with ultrasonic tips for a certain time. Then, this prepared dispersion is added to the primer material and mixed with an overhead stirrer at a certain time and speed. Finally, the mixture is soaking in an ultrasonic bath for 30 minutes before use to coat.



Figure 2.11: Primer and chemical conversion coated low carbon steel.

2.3. Polyamide Powder Preparation

Today, polyamides constitute an important part of the coating materials because of their commercial importance, versatility, and increasing number of applications [69]. PA12, one of these materials, was used as the topcoat layer in this study. Until this part of the study, chemical conversion and primer coating layer were applied on galvanized low carbon steel plates. The next process of this multilayer coating system is the topcoat layer. In this thesis, the powder form of PA12 is obtained from the bead form, to use in the preferred coating process. The purpose of this process was to be able to prepare a homogeneous rGO-PA12 dispersion in laboratory conditions. Therefore, the bead form of PA12 is exposed to some chemical and mechanical processes to obtain PA12 powder. The basic steps of these are described below.

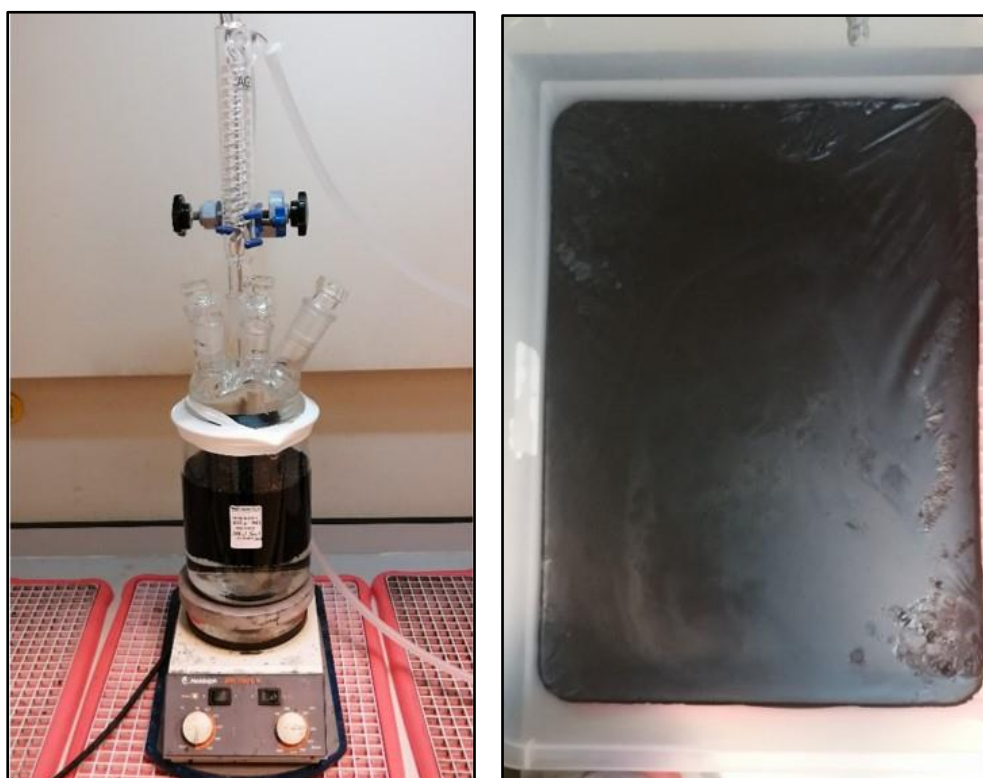


Figure 2.12: a) PA12 is melted in formic acid b) The melted PA12 is poured into a container.

First of all, it is necessary to start the process by melting the polyamide pieces which are in bead form. In this regard, the most suitable solvent that will not damage the PA12 is formic acid [70]. Through trial and error, we realized that the best scale to melt 1000 grams of polyamide in the form of beads added gradually is 1000 ml of formic acid at a certain temperature. So, this amount of PA12 and formic acid are added into a deep glass reactor which has a condenser on top of it. And then, the glass reactor is placed in a magnetic stirrer set at 350 °C and boiled for about 48 hours [71]. This step is shown in Figure 2.12 (a). These values vary according to the amount of the mixture and temperature, and they are obtained through experimentation. More polyamide pieces can be added to the mixture depends on the situation if the temperature value can be changed from time to time. The polyamide melted in a controlled manner is immediately poured into the large container before it solidifies and is spread over the entire container while still in the fluid form. Then it is left in the fume hood for about 2 days to dry completely and solidify as shown in Figure 2.12 (b). Occasionally, this drying time can be reduced by breaking up the solidified mixture into small pieces. Finally, they are grounded with the help of a mechanical grinder.

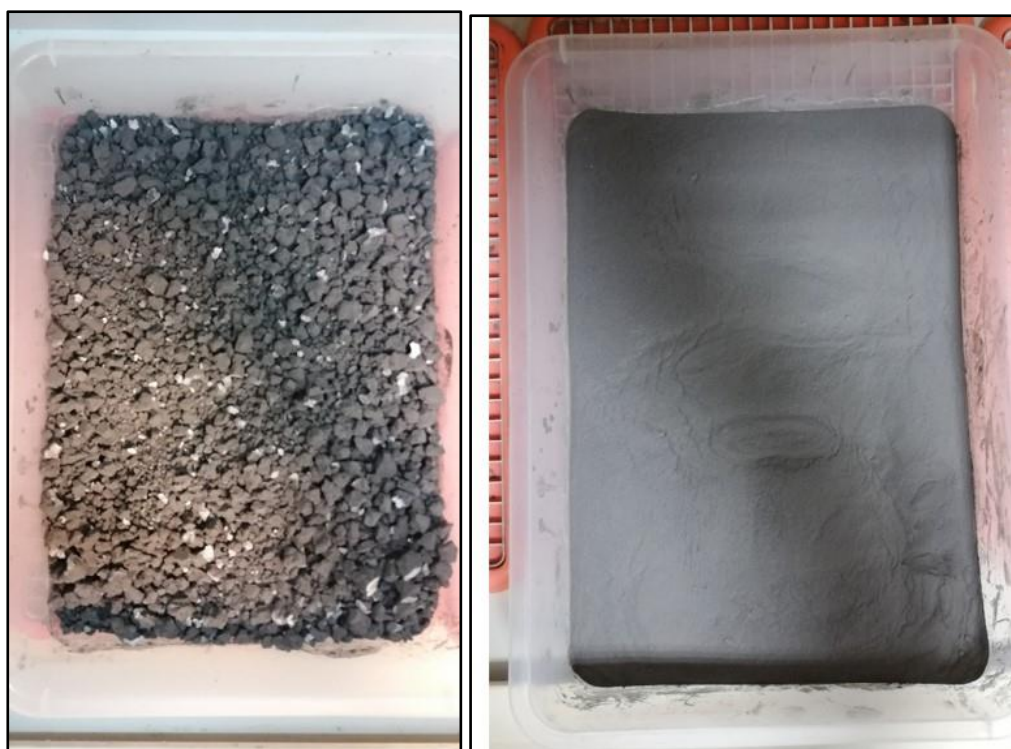


Figure 2.13: a) Dried PA12 b) Grounded PA12.

Since it is experienced that formic acid damages the primer material, which is the previous coating layer, the formic acid that was used to melt PA12 must be completely removed from the powder after the grinding process is completed. The ground polyamide is washed with ethanol to remove the formic acid. For this purpose, the polyamide mixed with approximately 1lt of ethanol is separated by first soaking in an ultrasonic bath for 2 h, and then by centrifuging at 8000 rpm for 5 minutes. This washing process with ethanol is repeated until the formic acid is completely removed, and It is left to dry at 60 °C in the oven [72]. Then, the same grinding processes are applied again. This time the polyamide powder is milled with a mechanical grinder until it is sieved through a 90-micron sieve. PA12 is now ready to use in our next coating process.



Figure 2.14: a) Separating ethanol from the mixture b) PA12/Water dispersion is prepared.

2.4. Polyamide 12 Coating

After obtaining a powder form of PA12, primer-coated samples are prepared for the topcoat. In pre-cleaning procedures, alcohol or acid is not used as well. Samples are washed with distilled water and cleaned by spraying the air with a compressor to avoid dust. The coating steps of PA12 are described below.

Firstly, the powder/water dispersion is prepared to distribute the powder particles homogeneously on the surface. Homogeneous polyamide-water dispersions with different ratios are prepared with the help of an ultrasonic homogenizer for about 24 hours. A certain amount of prepared dispersion is poured dropwise into the recess on the sample and waited until dispersion is spread by itself. At this stage, the important part is the samples are placed on a flat floor. Otherwise, the above-mentioned problems because of inhomogeneity may be encountered again. To avoid this situation, a working table with an adjustable inclination was designed, so that the floor is always stable and level. Shortly after the dispersion is spread through the cavity, the excess dispersion is discarded slowly and in a controlled manner with a doctor blade. This process is shown in Figure 2.15.

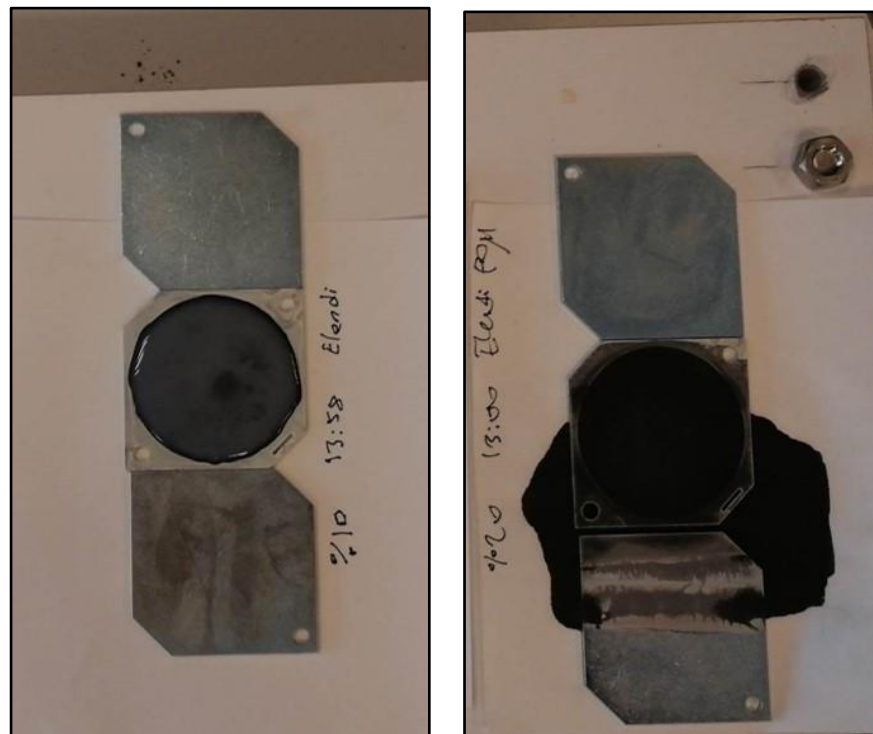


Figure 2.15: a) The dispersion is poured into recess b) The dispersion is spread.

The next step is the evaporation of the water in the dispersion, the melting of the powder particles in the recess, and finally the cooling process. For these steps, different drying, melting, and cooling processes were tried, and some parameters were determined according to the results obtained. Firstly, the sample is kept at room temperature for a while (2-3h) before putting it in the oven to let powder particles in the remaining dispersion collapse and the excess water on the dispersion evaporate. Then, the sample was tried to be coated with different temperature values and heating-cooling durations.

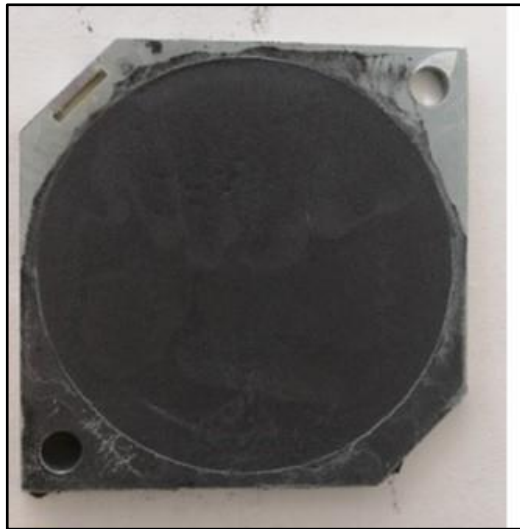


Figure 2.16: The excess dispersion is discarded.



Figure 2.17: The sample is dried in the oven.

Finally, the most successful coating was obtained by setting the oven set with 1°C/min ramp function, 300 min delay-off, from 20°C to 250°C. After 300 minutes, the sample is allowed to cool down inside before taking it out of the oven. As applied in chemical conversion and primer coating processes, the same coating steps are applied again on the once coated surface to completely get rid of the surface defects and obtained a more uniform and smooth coating. Figure 2.18 shows the examples of single layer and double layer PA12 coatings. Besides, these samples prepared with dispersions with different powder ratios (10%, 25%) were then compared and their effects on coating thickness were investigated.



Figure 2.18: a) Single-layer PA12 coating. b) Double-layer of PA12 coating.

3. MICROSTRUCTURE ANALYSIS

The microstructure and composition of polyamide-coated samples are analyzed with FT-IR, SEM, EDS methods. These methods help us to investigate the thicknesses of the layers, and they also provide some information about the composite of the coating and the surface topography.

The microstructures of the coatings were characterized by scanning electron microscopy. The SEM investigation was performed with a Philips XL 30 SFEG. The chemical composition was determined by energy-dispersive X-ray spectroscopy (SEM-EDS). FT-IR was carried out using PerkinElmer Spectrum 100 to identify and compare the chemical bonds in polyamide during different stages of the coating process.

Figure 3.1 represents the layers that we expected to observe galvanizing, chromium, conversion coating, primer, and PA12. As well as obtaining a multilayer coating, the thickness controllability, uniformity, microstructure of the composite are also important in this study.

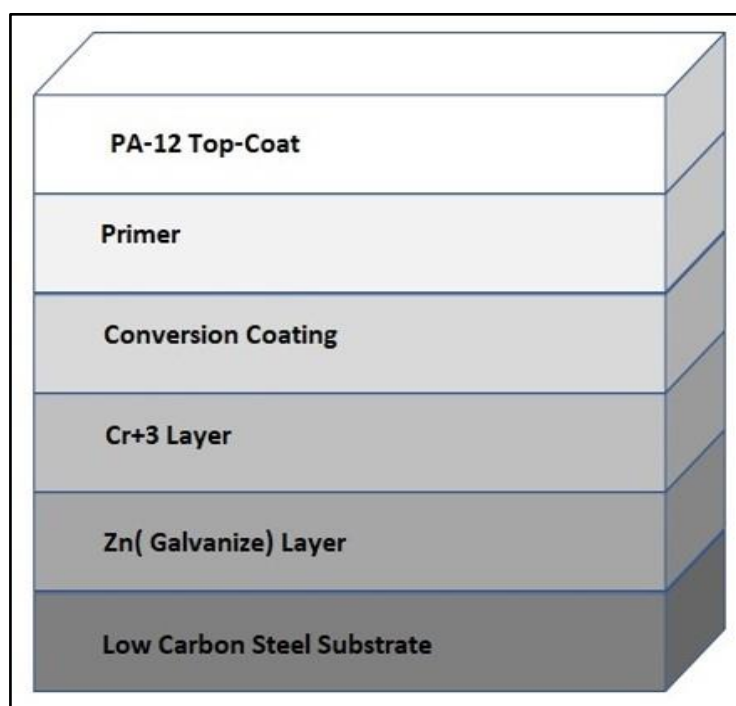


Figure 3.1: Coating layers.

Microstructure analyzes were made after the primer layer coating and the topcoat layer PA12 stages. The purpose of the analysis after the primer layer is to optimize the parameters of the newly developed granodine and primer coating methods and to obtain a controllable thickness. The purpose of the analysis after the topcoat layer is to examine the thickness variations and to extract the topology of the layers. Thickness analysis was performed for six samples coated with primer and six samples coated with a topcoat layer. These samples were coated using the same coating method and parameters.

Two sections were taken from each of the samples using a cut-off machine by Struers. Then, the sections were mounted in bakelite resin at 180 °C in 3 min by using Struers Labopress3 mounting equipment. This bakelite resin is shown in Figure 3.2. Then, the samples were wet ground with 80 to 1200 grain size grinding papers. A lubricant with high viscosity and cloths with high resilience was used for final polishing.



Figure 3.2: Mounted specimens in bakelite resin.

The samples are polished with aluminum oxide to obviate deformations and scratches after grinding papers. Thus, highly reflective surfaces are obtained for optical examination before SEM analysis. Before SEM analysis, the polished samples were also examined with an Olympus GX-50 optical microscope.

4. CORROSION TEST

The corrosion rate of the system is defined by the balance between two different reactions. These are the cathodic reaction which is the reduction of solution species and the anodic reaction which is the oxidation of the metal [73]. Some electrochemical testing methods can be used to measure the rate at which equilibrium is reached. In our study, we preferred to perform tests with the potentiodynamic polarization (Tafel plots) test method on the Gamry Interface 5000 E model as Figure 4.1 shows. In this type of measurement, we observe the overall change in the rate of reaction. A standard three-compartment cell used with graphite as the counter electrode, Ag/AgCl as the reference electrode, and our specimen as the working electrode. The cell is conducted on low carbon steel with different coatings in 3.5% wt. NaCl solution immersion. The exposing area for a specimen as the working electrode was calculated as 10 cm². The tests were carried out on four different samples. The averages of the corrosion rates of these samples were compared. All the corrosion experiments were carried out at the same temperature (20°C) and the open circuit potential and potentiodynamic for every specimen were performed for one time.

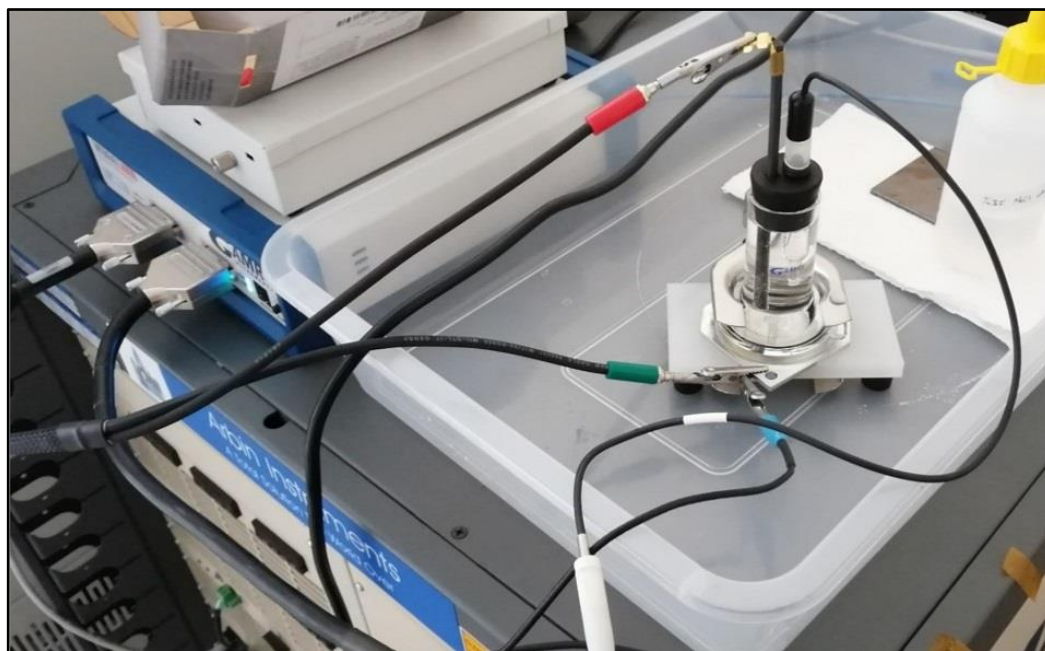


Figure 4.1: Corrosion test setup.

The open-circuit potential is the equilibrium potential assumed when no electrical connection is being applied to the system and, it was monitored continuously until the steady-state was reached, for about 4-6 hours. The cathodic and anodic potentiodynamic polarization measurements were then measured at a scan rate of 0.1 mV/s within a scan range of ± 250 mV. In Figure 4.2 where the vertical axis is the potential and the horizontal axis is the absolute current, anodic and cathodic currents are represented by two diverging logarithmic plot lines. The corrosion potential (E_{corr}) and corrosion current density (I_{corr}) are determined by the Tafel extrapolation technique from this curve that is a graphical relationship between current generated in an electrochemical cell and electrode potential [61]. After the potentiodynamic polarization curve is obtained, the Tafel curve is fit and the corrosion rate is calculated by Gamry Echem Analyst program [73].

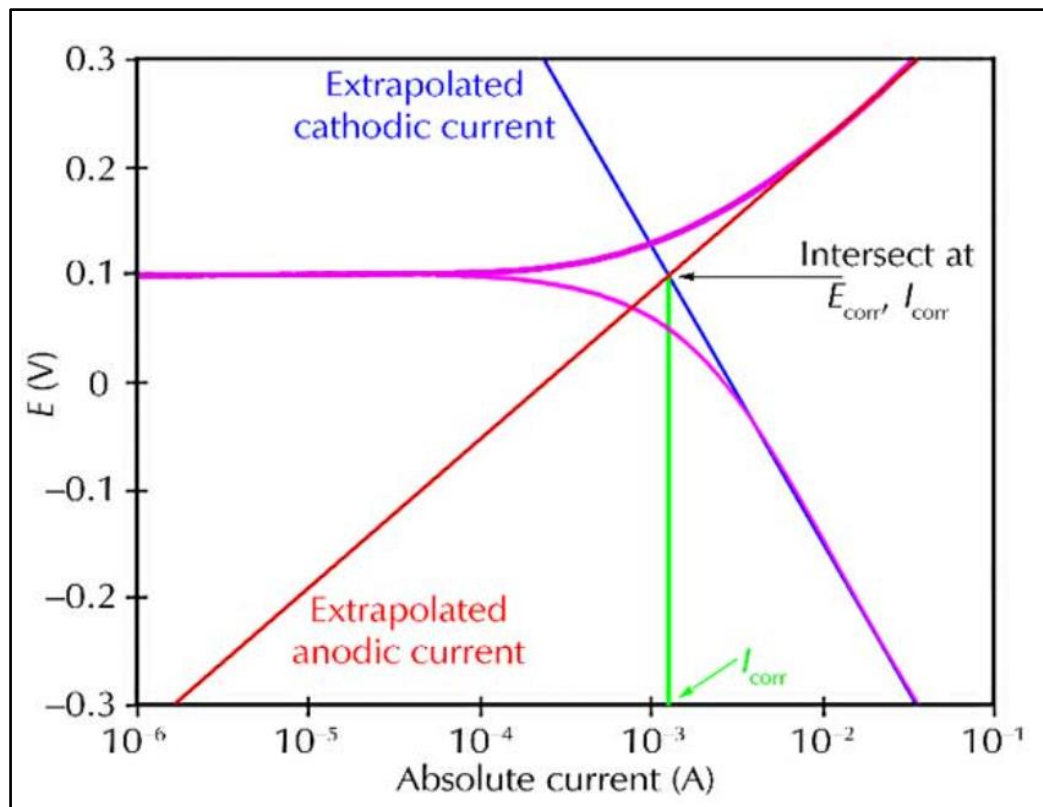


Figure 4.2: Corrosion process showing anodic and cathodic components of total current [73].

5. RESULTS AND DISCUSSIONS

One of the goals of this study is to obtain a multilayer polymer composite coating with uniform and controllable thicknesses. The multilayer coating system containing galvanization layer, chrome plating, chemical conversion layer, primer layer, and PA12 layer was successfully applied on a low carbon steel substrate. While obtaining this coating, many methods and tests were used, and the desired goals were achieved with a controlled thickness of the PA12 layer. Another goal of the study is to enhance the corrosion resistance of this multi-coating system by reinforcing graphene-based material into the primer layer. In this regard, considerable improvement has been observed. The results obtained from the experiments and tests conducted in line with these purposes are shared below.

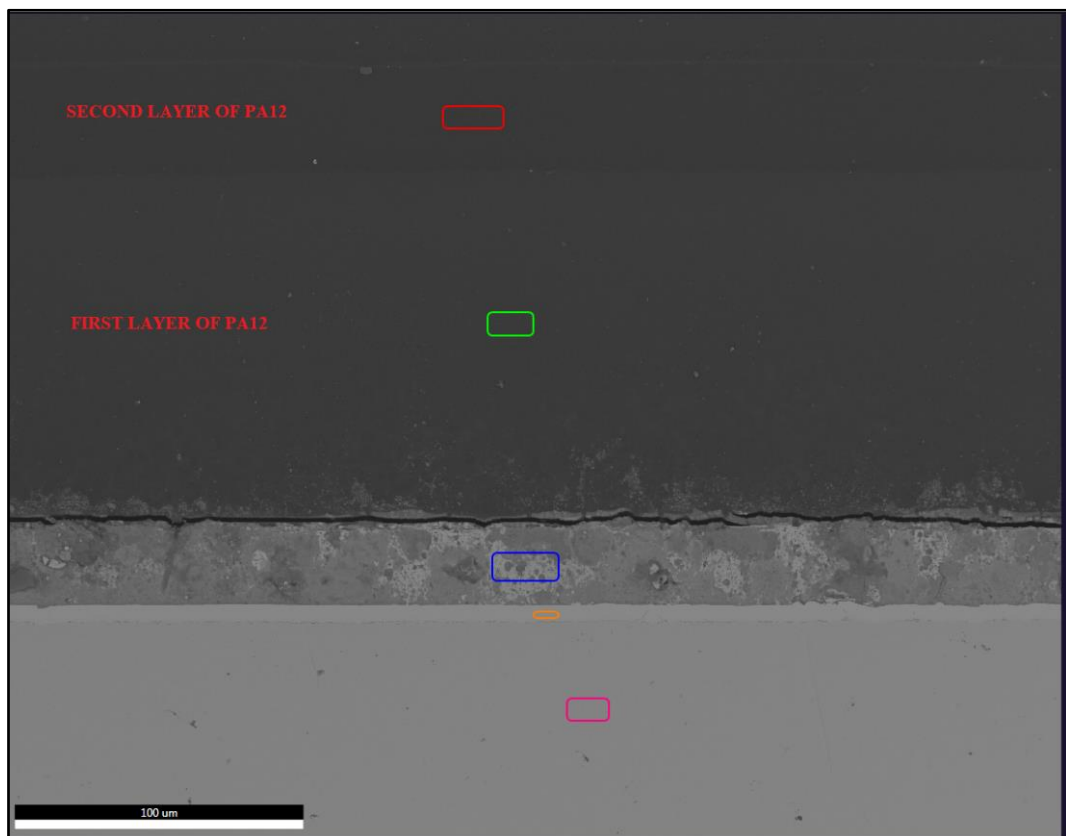


Figure 5.1: Chemical composition with SEM-EDS.

In Figure 5.1, showing the chemical composition of the multilayer coating system, EDS analysis was performed for 5 different selected areas. Each coating layer was determined according to the presence of the element's strong peaks in the results. Based on these results, it was observed that diffusion occurred between the granodine and primer layers, so the transition between these layers was not fully determined.

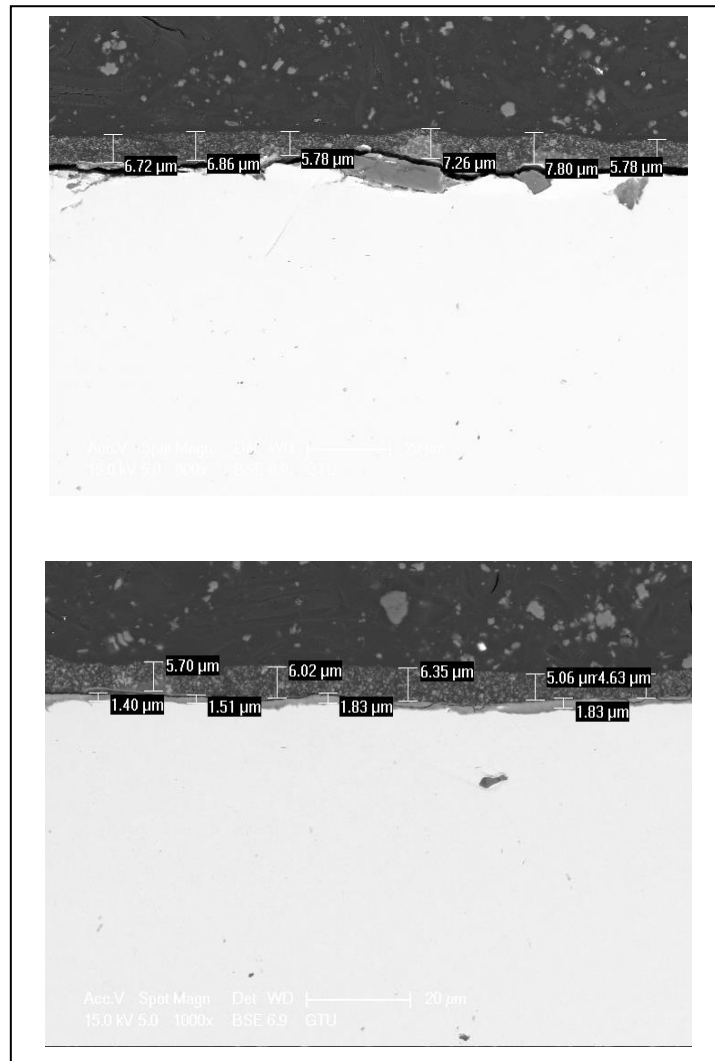


Figure 5.2: SEM results of primer-coated samples.

According to the SEM results, the parameters of the technique to be used in the primer coating process are determined. Desired coating results are obtained when 75% wt of primer is used and the coating process is applied twice. As can be seen in Figure 5.2, the thickness of the primer coating layer on granodine is stable. It is

observed that the thickness variation of the primer coating layer is acceptable. At the same time, it is calculated that the average thickness of the primer layer is $\pm 6,1 \mu\text{m}$.

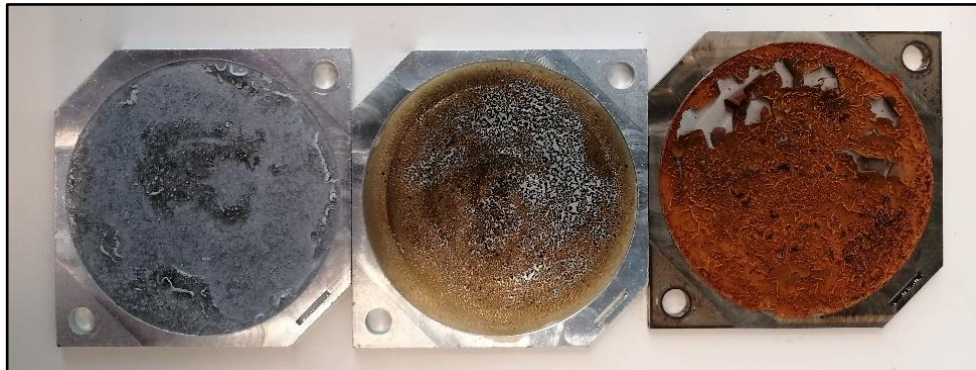


Figure 5.3: Coating failures.

For PA12 coating, the PA12 powders were perfused directly into the recess and they were expected to spread evenly while melting. Then, experiments were carried out on the cooling-heating rates and the maximum temperature of the oven was set to improve the quality of the coating. As a result of all these experiments, pinholes, flaking, and runs were observed due to the non-homogeneous distribution of PA12 powders. Some coatings failures were obtained when PA12 powders were not dispersed with the help of PA12/water dispersion as shown in Figure 5.3. Then, homogeneous polyamide-water dispersions with different ratios are prepared with the help of an ultrasonic homogenizer for about 24 hours, and homogeneous distribution was achieved.

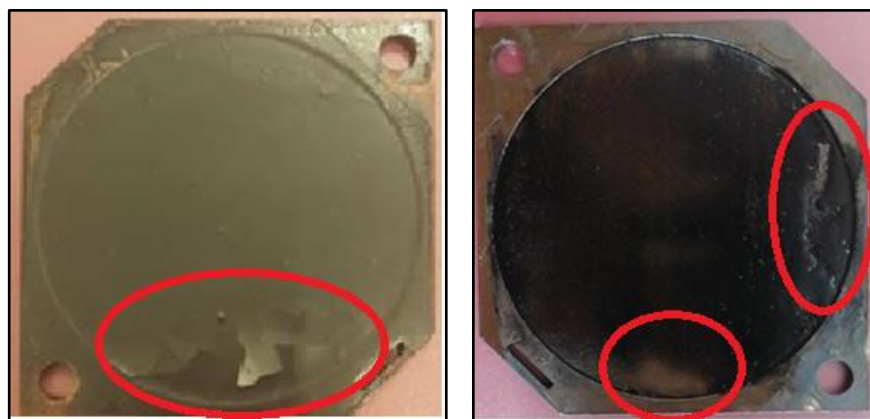


Figure 5.4: Coating failures.

Other coating failures prepared at different furnace regimes and dispersion concentrations while performing PA12 coating studies were also shown in Figure 5.4. In this regard, a range of 200°C to 250°C was tried for the maximum temperature of the oven. And, a range of 5% to 20% was tested for the PA12/water dispersion concentration. Then, the most successful coating was obtained by setting the oven set with 1°C/min ramp function, 300 min delay-off, from 20°C to 250°C when 20% PA12/water dispersion was used.

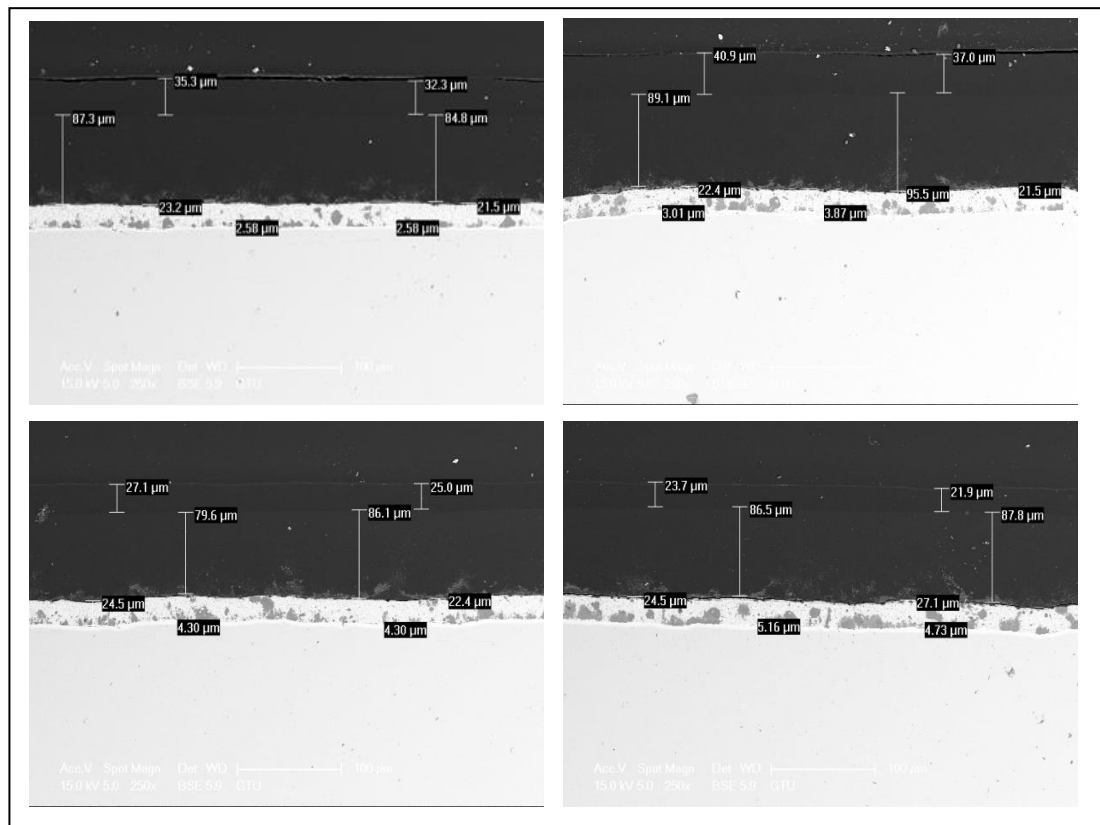


Figure 5.5: SEM results of 4 different sample sections.

In Figure 5.5, SEM results of coating samples are showed. These results belong to the sections taken from 4 different samples coated with the same methods. All top coatings were prepared with 20% PA12/water dispersion. The coating processes of the other layers were also carried out with the same methods and equipment for each sample. The SEM results support that the thickness change of the second layer of PA12 for each same sample is $\pm 2 \mu\text{m}$. It proves that uniform thickness is obtained for the second layer of PA12 coatings throughout all sample surfaces. At the same time, it was calculated that the average thickness of the second layer of PA12 coatings was

30.4 μm and its standard deviation was 7 μm for all samples. It proves that the differences in layer thickness between the different samples were low. It is obvious a multi-layer coating with a stable coating thickness can be achieved with the newly developed coating methods in this work.

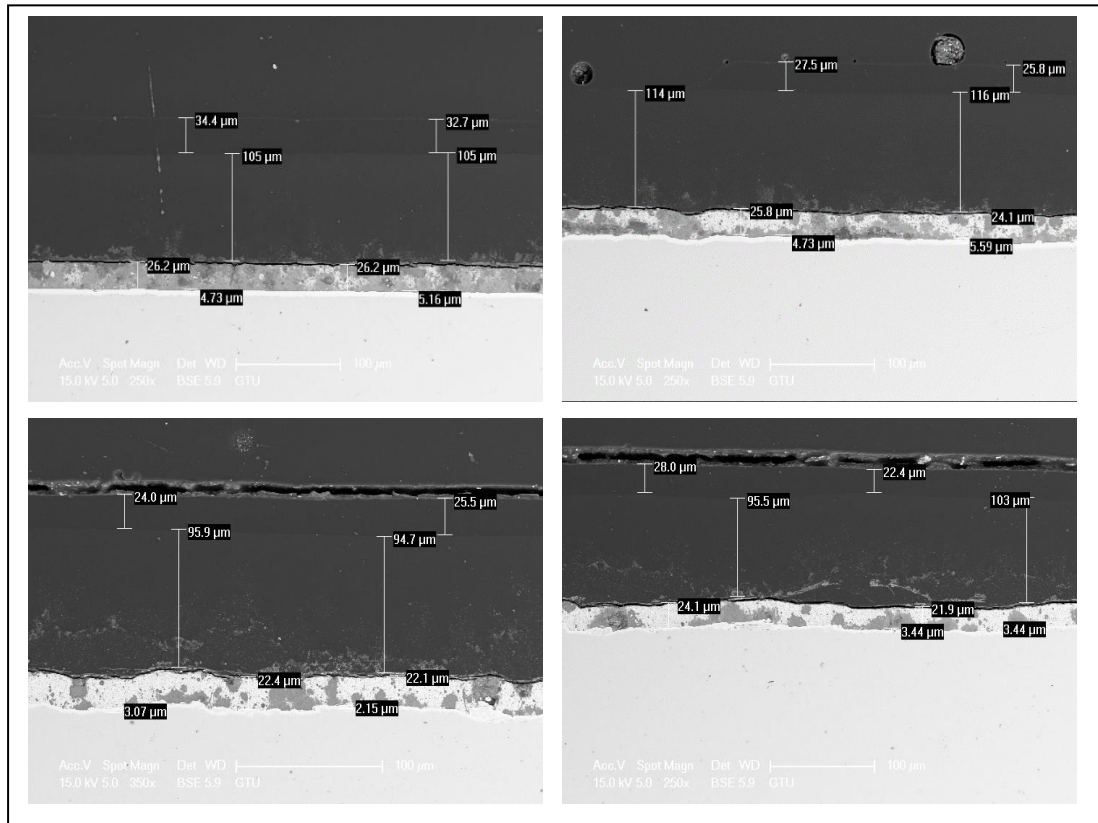


Figure 5.6: SEM results of 4 different sample sections with different dispersion ratios.

At the same time, the effect of process parameters on coating thickness is examined. The results in Figure 5.6 are obtained from samples that are prepared using the different process parameters and are compared to the previous results in Figure 5.5. Two sections are taken from samples that are obtained by using 10% PA/water dispersion for the first layers of PA12 coating. Their SEM results are shown in Figure 5.6. As expected, reasonable differences in the first-layer thickness values of PA12 coating are noticed compared to previous samples shown in Figure 5.5. While the average thickness of the coating prepared with a 20% dispersion ratio is 87 μm , the average thickness of the coating prepared with a 10% dispersion ratio is measured as 101.3 μm . It shows that coating thickness can be controlled by changing the parameters in the coating processes and the desired thickness can be obtained.

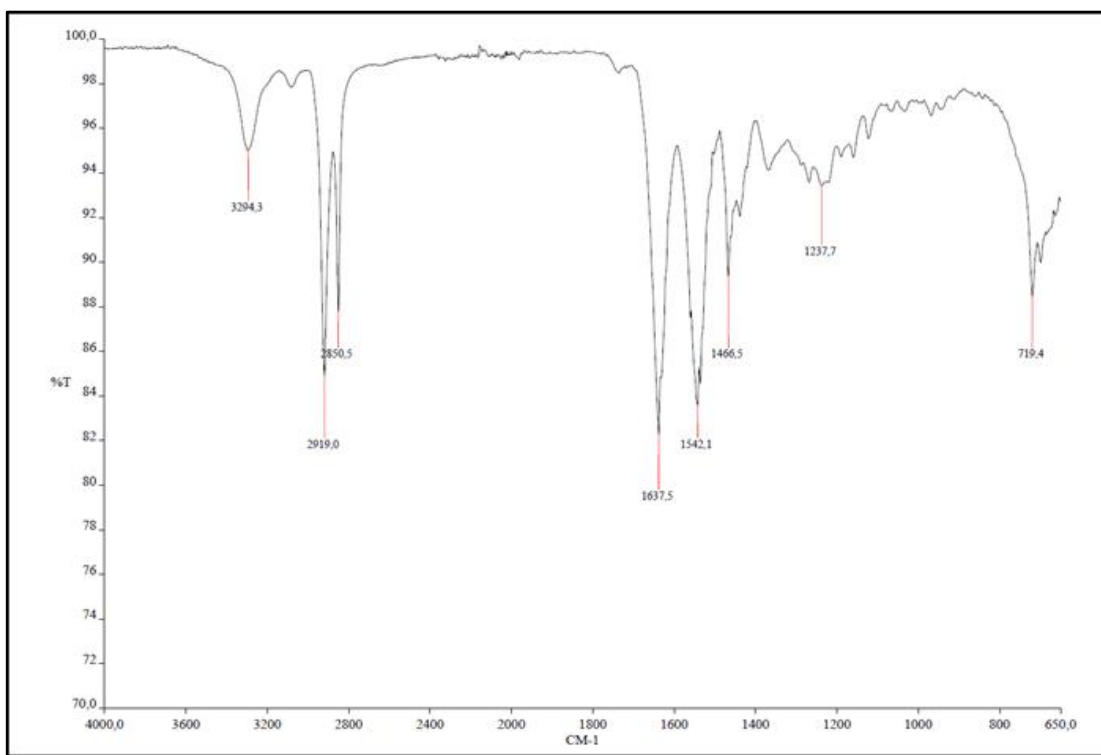


Figure 5.7: FT-IR patterns (A) melted PA12.

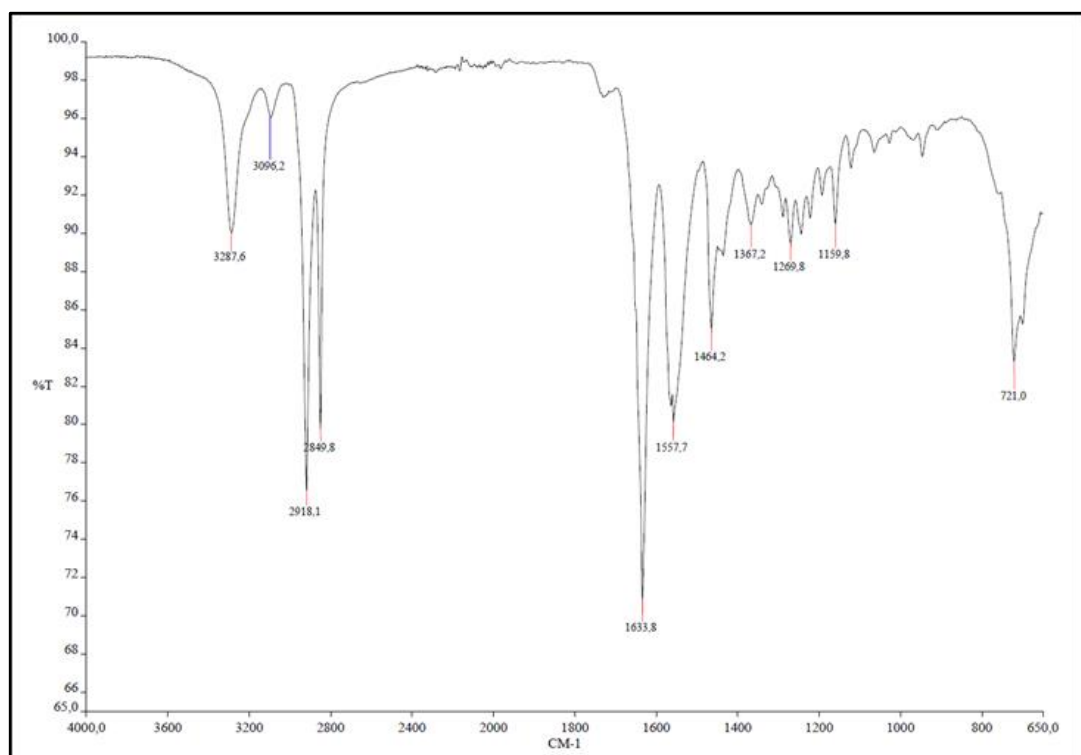


Figure 5.8: FT-IR patterns (B) dissolved PA12 in formic acid.

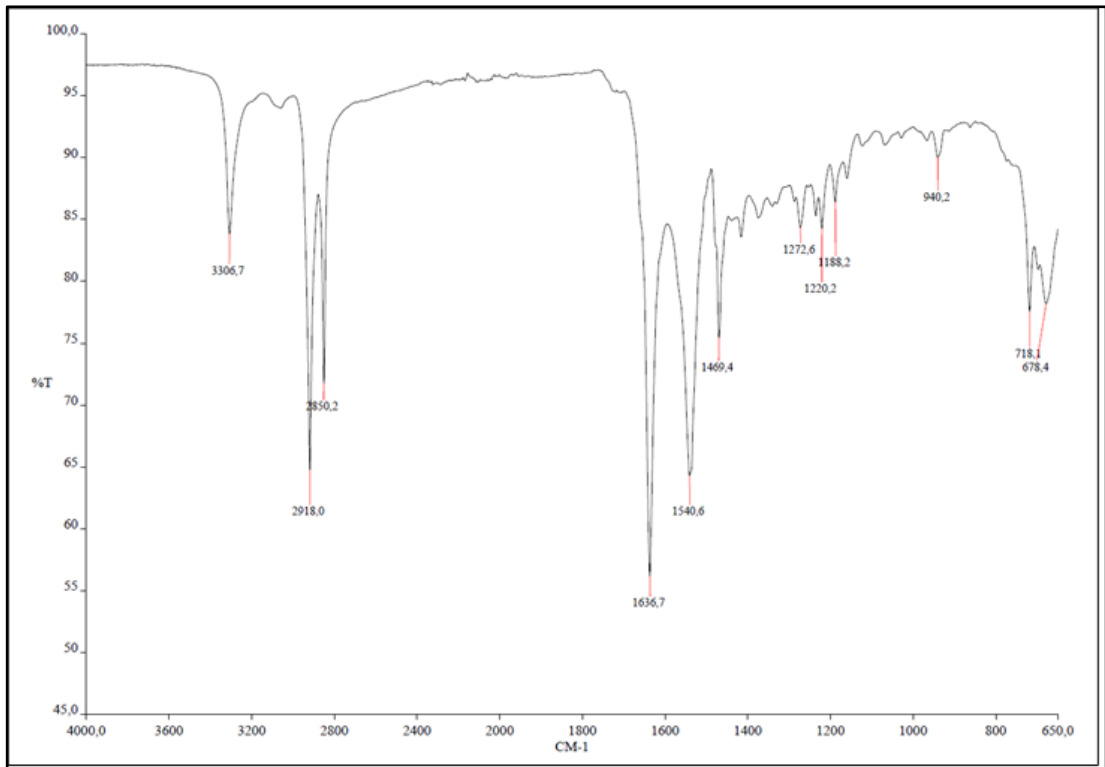


Figure 5.9: FT-IR patterns (C) washed PA12 in ethanol.

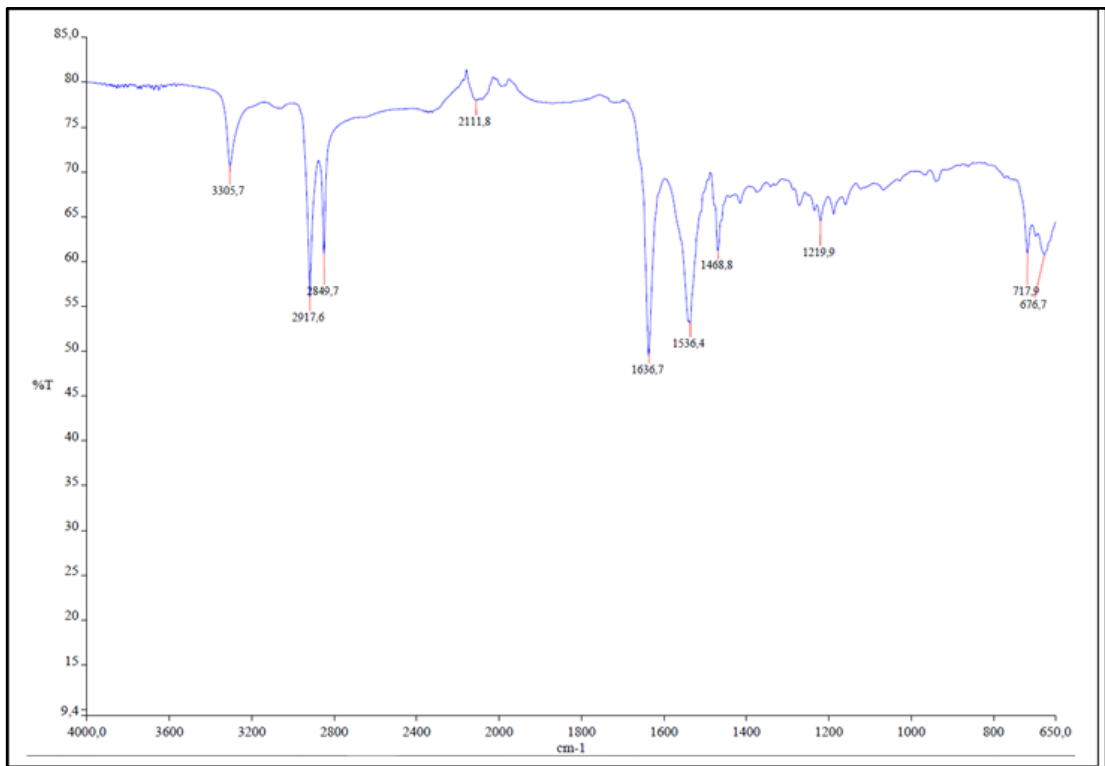


Figure 5.10: FT-IR patterns (D) RGO-PA12 composite.

FT-IR analysis is performed to compare the PA12 powder form obtained with the untreated PA12 bead form. FT-IR results of specimens taken from some stages of the PA12 powder preparation process are also compared. FT-IR results of melted PA12, dissolved PA12 in formic acid, washed PA12 in ethanol, and RGO-PA12 composite are shown in Figure 5.7, Figure 5.8, Figure 5.9, and Figure 5.10, respectively. These results suggest that there is no differentiation in terms of the type of functional groups. It is seen that bonds belonging to functional groups preserve their existence.

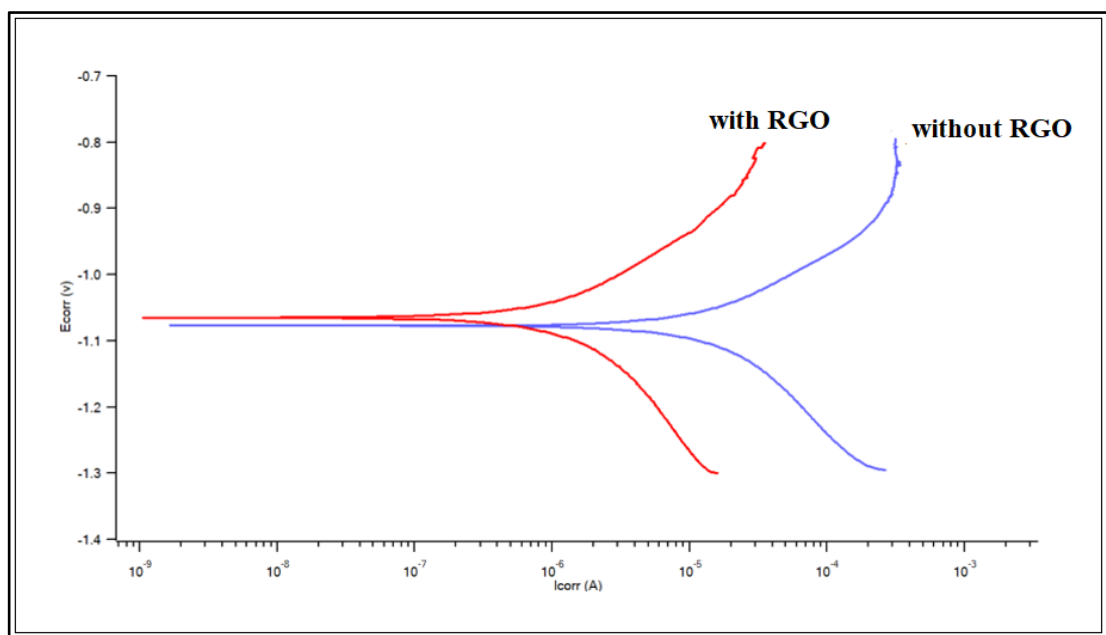


Figure 5.11: Tafel polarization curves.

The corrosion performance of the prepared samples was investigated with Tafel Method. The red line in Figure 5.11 represents the polarization curve results of the graphene-based polymer coatings. The blue line represents the results of polymer coatings that do not include graphene derivatives. The corrosion protection of the samples was estimated from the values of E_{corr} and I_{corr} , which were calculated from the Tafel polarization curves. According to this graph, we observe a decrease in corrosion density and an increase in corrosion potential as expected. The polarization curves of RGO composite coated steel show a significant shift of corrosion density to more negative values compared to coating without RGO, confirming thereby that

RGO composite coated steel has much better corrosion resistance compared to the composite coating which has not include RGO. In other words, the RGO composite coated samples have also a bigger corrosion potential, indicating that the RGO coated sample forms a strong protective layer and improves the corrosion resistance of the steel.

Table 5.1 Corrosion test results.

Sample	Average Corrosion Rate (mm/year)
Composite coating without RGO	16,805x10 ⁻³
Composite coating with RGO	1,6608x10 ⁻³

From the overall results of the Tafel plot, Table 5.1 summarizes the average corrosion rates of reduced GO composite coatings and composite coatings without reduced GO. This clearly shows that reduced GO composite coated steel reduces the corrosion rate from 16,805x10⁻³ mm/year to 1,6608x10⁻³ mm/year. The reduction in the corrosion rate of reduced graphene oxide coated low carbon steel is 10 times compared to composite coating without reduced GO.

6. CONCLUSIONS AND FUTURE WORKS

In this thesis, a novel and stable graphene reinforced polymer composite coating has been successfully fabricated on low carbon steel. A new coating method has also been developed to create crack-free, uniform, corrosion-resistant polymer composite coating with controlled and uniform thickness on low carbon steel. This developed graphene reinforced polymer composite coating can be an alternative protection method against corrosion for some engineering applications. This new coating method may throw light on future experimental researches and industrial applications. The electrochemical measurements further establish that reduced graphene oxide helps the surface to protect from corrosion when immersed in a 3.5% wt. NaCl solution. The corrosion resistance is observed to be 10 times better.

In near future, the mechanical characterization of coatings with and without RGO may be analyzed with run scratch and nanoindentation tests. Also, the effects of RGO addition on bonding quality in different coating layers can be investigated and the corrosion resistance of coatings containing different ratios and derivatives of graphene can also be compared.

The effects of reduced graphene oxide addition on different layers for improved performance of the systems without significant cost increase with superior performance boosts of graphene addition may also be investigated. In addition to that thinner coatings with similar or better performance may be manufactured and the thickness of the layers may be optimized for cheaper coatings applications.

7. PUBLICATIONS FROM THESIS

- [1] S. B. Akturk, R. Önler, E. Topac, E. Ozdemir, A. S. Oktem, and O. B. Saban, (2020). “Enhancing Corrosion Resistance of Steel Substrates with Reduced Graphene Oxide Reinforced Polymer Composite Coatings,” presented at the Materials Science&Technology MST2020.

REFERENCES

- [1] Li, J., Cui, J., Yang, J., Li, Y., Qiu, H., & Yang, J. (2016). Reinforcement of graphene and its derivatives on the anticorrosive properties of waterborne polyurethane coatings. *Composites Science and Technology*, 129, 30-37.
- [2] Roberge, P. R. (2008). *Corrosion engineering principles and practice*. McGraw-Hill.
- [3] Chen, S., Brown, L., Levendorf, M., Cai, W., Ju, S., & Edgeworth, J. et al. (2011). Oxidation Resistance of Graphene-Coated Cu and Cu/Ni Alloy. *ACS Nano*, 5(2), 1321-1327.
- [4] M. G. Fontana and N. D. Greene, "Corrosion Engineering", Chapter 3, McGraw-Hill, New York (1978).
- [5] Averill, B., & Eldredge, P. (2013). *General chemistry: principles, patterns, and applications*. Flat World Knowledge, Inc.
- [6] Council, National & Sciences, Division & Board, National & Engineering, Committee. (2011). *Research Opportunities in Corrosion Science and Engineering*.
- [7] Corrosion - Wikipedia. (2021). Retrieved 7 May 2021, from <https://en.wikipedia.org/wiki/Corrosion>.
- [8] Koch, G., Brongers, M., Thompson, N., Virmani, Y., & Payer, J. (2002). Corrosion cost and preventative strategies in the United States. Retrieved 7 May 2021, from <https://trid.trb.org/view/707382>.
- [9] Çakır, A.F. (2016). Korozyon: insanlık için stratejik öneme sahip tabii bir olay. Retrieved 7 May 2021, from https://www.metalurji.org.tr/dergi/dergi179/d179_3540.pdf.
- [10] Cui, G., Bi, Z., Zhang, R., Liu, J., Yu, X., & Li, Z. (2019). A comprehensive review on graphene-based anti-corrosive coatings. *Chemical Engineering Journal*, 373, 104-121.
- [11] Othman, N., Che Ismail, M., Mustapha, M., Sallih, N., Kee, K., & Ahmad Jaal, R. (2019). Graphene-based polymer nanocomposites as barrier coatings for corrosion protection. *Progress In Organic Coatings*, 135, 82-99.
- [12] Graphene Coating Promises to Improve Condenser Efficiency. *Focus on Powder Coatings*, 2015. 2015(8): p. 5.
- [13] Sørensen, P.A., et al., Anticorrosive coatings: a review. *Journal of Coatings Technology and Research*, 2009. 6(2): p. 135-176.

- [14] Mahajan, S. (2001). Encyclopedia of materials: science and technology. Elsevier.
- [15] S.Covino, B., Cramer, S. D., Covino, J., & S., B. (2003). ASM Handbook: Corrosion: Fundamentals, Testing, and Protection (10th ed.). ASM International.
- [16] Hernández-Padrón, G., Rojas, F., & Castaño, V. (2006). Development and testing of anticorrosive SiO₂/phenolic–formaldehyde resin coatings. Surface and Coatings Technology, 201(3-4), 1207-1214.
- [17] Alhumade, H., et al., Corrosion inhibition of copper in sodium chloride solution using polyetherimide/graphene composites. The Canadian Journal of Chemical Engineering, 2016. 94(5): p. 896-904.
- [18] Liu, J., Yu, Q., Yu, M., Li, S., Zhao, K., Xue, B., & Zu, H. (2018). Silane modification of titanium dioxide-decorated graphene oxide nanocomposite for enhancing anticorrosion performance of epoxy coatings on AA-2024. Journal Of Alloys And Compounds, 744, 728-739.
- [19] Liu, T., Liu, Y., Ye, Y., Li, J., Yang, F., Zhao, H., & Wang, L. (2019). Corrosion protective properties of epoxy coating containing tetraaniline modified nano- α -Fe₂O₃. Progress In Organic Coatings, 132, 455-467.
- [20] Saravanan, P., Jayamoorthy, K., & Ananda Kumar, S. (2016). Design and characterization of non-toxic nano-hybrid coatings for corrosion and fouling resistance. Journal Of Science: Advanced Materials And Devices, 1(3), 367-378.
- [21] Asaldoust, S., & Ramezanzadeh, B. (2020). Synthesis and characterization of a high-quality nanocontainer based on benzimidazole-zinc phosphate (ZP-BIM) tailored graphene oxides; a facile approach to fabricating a smart self-healing anti-corrosion system. Journal Of Colloid And Interface Science, 564, 230-244.
- [22] Taheri, N., Ramezanzadeh, B., & Mahdavian, M. (2019). Application of layer-by-layer assembled graphene oxide nanosheets/polyaniline/zinc cations for construction of an effective epoxy coating anti-corrosion system. Journal Of Alloys And Compounds, 800, 532-549.
- [23] Javidparvar, A., Naderi, R., & Ramezanzadeh, B. (2020). Manipulating graphene oxide nanocontainer with benzimidazole and cerium ions: Application in epoxy-based nanocomposite for active corrosion protection. Corrosion Science, 165, 108379.
- [24] Ramezanzadeh, B., Shamshiri, M., & Ganjaee Sari, M. (2018). Designing a multi-functionalized clay lamellar-co-graphene oxide nanosheet system: An inventive approach to enhance mechanical characteristics of the corresponding epoxy-based nanocomposite coating. Progress In Organic Coatings, 116, 7-20.

- [25] Mohammadkhani, R., Ramezanzadeh, M., Saadatmandi, S., & Ramezanzadeh, B. (2020). Designing a dual-functional epoxy composite system with self-healing/barrier anti-corrosion performance using graphene oxide nano-scale platforms decorated with zinc doped-conductive polypyrrole nanoparticles with great environmental stability and non-toxicity. *Chemical Engineering Journal*, 382, 122819.
- [26] Ramezanzadeh, M., Ramezanzadeh, B., Mahdavian, M., & Bahlakeh, G. (2020). Development of metal-organic framework (MOF) decorated graphene oxide nanoplateforms for anti-corrosion epoxy coatings. *Carbon*, 161, 231-251.
- [27] Graphene – Wikipedia. (2021). Retrieved 1 June 2021, from <https://en.wikipedia.org/wiki/Graphene>.
- [28] Graphenea. (2018, July 04). Differences Between Graphene and Graphite. AZoNano. Retrieved on June 03, 2021, from <https://www.azonano.com/article.aspx?ArticleID=3836>.
- [29] Liu, S., Chevali, V., Xu, Z., Hui, D., & Wang, H. (2018). A review of extending performance of epoxy resins using carbon nanomaterials. *Composites Part B: Engineering*, 136, 197-214.
- [30] Tan, B., & Thomas, N. (2016). A review of the water barrier properties of polymer/clay and polymer/graphene nanocomposites. *Journal Of Membrane Science*, 514, 595-612.
- [31] Novoselov, K. (2004). Electric Field Effect in Atomically Thin Carbon Films. *Science*, 306(5696), 666-669.
- [32] Novoselov, K., Geim, A., Morozov, S., Jiang, D., Katsnelson, M., & Grigorieva, I. et al. (2005). Two-dimensional gas of massless Dirac fermions in graphene. *Nature*, 438(7065), 197-200.
- [33] Balandin, A., Ghosh, S., Bao, W., Calizo, I., Teweldebrhan, D., Miao, F., & Lau, C. (2008). Superior Thermal Conductivity of Single-Layer Graphene. *Nano Letters*, 8(3), 902-907.
- [34] Lee, C., Wei, X., Kysar, J., & Hone, J. (2008). Measurement of the Elastic Properties and Intrinsic Strength of Monolayer Graphene. *Science*, 321(5887), 385-388.
- [35] Chen, Z. (2001). A mechanical assessment of flexible optoelectronic devices. *Thin Solid Films*, 394(1-2), 201-205.
- [36] Ramanathan, T., Abdala, A., Stankovich, S., Dikin, D., Herrera-Alonso, M., & Piner, R. et al. (2008). Functionalized graphene sheets for polymer nanocomposites. *Nature Nanotechnology*, 3(6), 327-331.

- [37] Villar-Rodil, S., Paredes, J., Martínez-Alonso, A., & Tascón, J. (2009). Preparation of graphene dispersions and graphene-polymer composites in organic media. *Journal Of Materials Chemistry*, 19(22), 3591.
- [38] Wang, S., Lin, W., Ceng, S., & Zhang, J. (1998). Corrosion Inhibition of Reinforcing Steel by Using Acrylic Latex 11Communicated by D.M. Roy. *Cement and Concrete Research*, 28(5), 649-653.
- [39] Sekine, I., Yuasa, M., Hirose, N., & Tanaki, T. (2002). Degradation evaluation of corrosion protective coatings by electrochemical, physicochemical, and physical measurements. *Progress In Organic Coatings*, 45(1), 1-13.
- [40] Liu, X., Xiong, J., Lv, Y., & Zuo, Y. (2009). Study on corrosion electrochemical behavior of several different coating systems by EIS. *Progress In Organic Coatings*, 64(4), 497-503.
- [41] Wang, X., et al., Graphene Reinforced Composites as Protective Coatings for Oil and Gas Pipelines. *Nanomaterials (Basel)*, 2018. 8(12).
- [42] Kozhukharov, S., Samichkov, V., Girginov, C., & Machkova, M. (2017). Actual trends in the elaboration of advanced multifunctional coating systems for the efficient protection of lightweight aircraft alloys. *Corrosion Reviews*, 35(6), 383-396.
- [43] Galvão, T., Wilhelm, M., Gomes, J., & Tedim, J. (2020). Emerging trends in smart nanocontainers for corrosion applications. *Smart Nanocontainers*, 385-398.
- [44] Nine, M., Cole, M., Tran, D., & Losic, D. (2015). Graphene: a multipurpose material for protective coatings. *Journal Of Materials Chemistry A*, 3(24), 12580-12602.
- [45] Kang, D., Kwon, J., Cho, H., Sim, J., Hwang, H., & Kim, C. et al. (2012). Oxidation Resistance of Iron and Copper Foils Coated with Reduced Graphene Oxide Multilayers. *ACS Nano*, 6(9), 7763-7769.
- [46] Prasai, D., Tuberquia, J., Harl, R., Jennings, G., & Bolotin, K. (2012). Graphene: corrosion-inhibiting Coating. *ACS Nano*, 6(2), 1102-1108.
- [47] F., Camilli, L., Wang, T., Mackenzie, D., Curioni, M., Akid, R., & Bøggild, P. (2018). Complete long-term corrosion protection with chemical vapor deposited graphene. *Carbon*, 132, 78-84.
- [48] Olia, H., Ghobadi, M., Danaee, I., & Onsoni, S. (2020). Effect of number of layers on erosion, corrosion, and wear resistance of multilayer Cr–N/Cr–Al–N coatings on AISI 630 stainless steel. *Materials And Corrosion*, 71(8), 1361-1374.
- [49] Tiwari, A., & Singh Raman, R. (2017). Durable Corrosion Resistance of Copper Due to Multi-Layer Graphene. *Materials*, 10(10), 1112.

- [50] Ramezanzadeh, B., Mohamadzadeh Moghadam, M., Shohani, N., & Mahdavian, M. (2017). Effects of highly crystalline and conductive polyaniline/graphene oxide composites on the corrosion protection performance of a zinc-rich epoxy coating. *Chemical Engineering Journal*, 320, 363-375.
- [51] Liu, D., Zhao, W., Liu, S., Cen, Q., & Xue, Q. (2016). Comparative tribological and corrosion resistance properties of epoxy composite coatings reinforced with functionalized fullerene C60 and graphene. *Surface And Coatings Technology*, 286, 354-364.
- [52] Ding, R., Zheng, Y., Yu, H., Li, W., Wang, X., & Gui, T. (2018). Study of water permeation dynamics and anti-corrosion mechanism of graphene/zinc coatings. *Journal Of Alloys And Compounds*, 748, 481-495.
- [53] Zhou, S., Wu, Y., Zhao, W., Yu, J., Jiang, F., Wu, Y., & Ma, L. (2019). Designing reduced graphene oxide/zinc rich epoxy composite coatings for improving the anticorrosion performance of carbon steel substrate. *Materials & Design*, 169, 107694.
- [54] Singh, B., Nayak, S., Nanda, K., Jena, B., Bhattacharjee, S., & Besra, L. (2013). The production of corrosion-resistant graphene reinforced composite coating on copper by electrophoretic deposition. *Carbon*, 61, 47-56.
- [55] Sun, W., Wang, L., Wu, T., Pan, Y., & Liu, G. (2015). Inhibited corrosion-promotion activity of graphene encapsulated in nanosized silicon oxide. *Journal Of Materials Chemistry A*, 3(32), 16843-16848.
- [56] Bunch, J., Verbridge, S., Alden, J., van der Zande, A., Parpia, J., Craighead, H., & McEuen, P. (2008). Impermeable Atomic Membranes from Graphene Sheets. *Nano Letters*, 8(8), 2458-2462.
- [57] Singhababu, Y., Sivakumar, B., Choudhary, S., Das, S., & Sahu, R. (2018). Corrosion-protective reduced graphene oxide coated cold rolled steel prepared using industrial setup: A study of protocol feasibility for commercial production. *Surface And Coatings Technology*, 349, 119-132.
- [58] Chang, C., Huang, T., Peng, C., Yeh, T., Lu, H., & Hung, W. et al. (2012). Novel anticorrosion coatings prepared from polyaniline/graphene composites. *Carbon*, 50(14), 5044-5051.
- [59] Yu, Y., Lin, Y., Lin, C., Chan, C., & Huang, Y. (2014). High-performance polystyrene/graphene-based nanocomposites with excellent anti-corrosion properties. *Polym. Chem.*, 5(2), 535-550.
- [60] Cho J, Gao L, Tian J, Cao H, Wu W, Yu Q. Atomic-scale investigation of graphene grown on Cu foil and the effects of thermal annealing. *ACS Nano*. 2011; 5: 3607-3613.

- [61] Podila, R., Moore, T., Alexis, F., & Rao, A. (2013). Graphene Coatings for Biomedical Implants. *Journal Of Visualized Experiments*, (73).
- [62] Zhang, W., Lee, S., McNear, K., Chung, T., Lee, S., & Lee, K. et al. (2014). Use of graphene as protection film in biological environments. *Scientific Reports*, 4(1).
- [63] Double Wall Tubes - Bantboru. (2021). Retrieved 7 May 2021, from <http://www.bantboru.com/cift-katli-borular/EN>.
- [64] Hughes, A. (2018). Conversion Coatings. *Encyclopedia Of Interfacial Chemistry*, 108-114.
- [65] Hesamedini, S., & Bund, A. (2019). Trivalent chromium conversion coatings. *Journal Of Coatings Technology And Research*, 16(3), 623-641.
- [66] Bonderite M-NT 1455T. (2021). Retrieved 7 May 2021, from https://www.henkel-adhesives.com/fr/en/product/surface-post-treatments/bonderite_m-nt_1455t.html.
- [67] Narayanan, T. S. N. S. (2005). Surface Pretreatment by Phosphate Conversion Coatings-A Review. *Rev. Adv. Mater. Sci.*, 9 (2), 130–177.
- [68] Enhancement of adhesion [SubsTech] . (2021). Retrieved 7 May 2021, from https://www.substech.com/dokuwiki/doku.php?id=enhancement_of_adhesion
- [69] Marchildon, K. (2010). Polyamides - Still Strong After Seventy Years. *Macromolecular Reaction Engineering*, 5(1), 22-54.
- [70] Behler, K., Havel, M., & Gogotsi, Y. (2007). New solvent for polyamides and its application to the electrospinning of polyamides 11 and 12. *Polymer*, 48(22), 6617-6621.
- [71] Nylon 12 (PA 12). (2012). *Chemical Resistance Of Thermoplastics*, 1813-1874.
- [72] Ethanol, MSDS No.322415 [Online], Retrieved 7 May 2021, from <https://www.sigmaaldrich.com/>.
- [73] Electrochemical Corrosion Measurements-Galvanic Corrosion. (2021). Retrieved 7 May 2021, from <https://www.gamry.com/application-notes/corrosion-coatings/basics-of-electrochemical-corrosion-measurements/>.

BIOGRAPHY

Samet Berk AKTÜRK graduated from Mechanical Engineering of Abdullah Gül University in 2018, He received his Master of Science degree in Mechanical Engineering from Gebze Technical University Graduate School of Natural and Applied Sciences in 2021.